Master's thesis

NTNU
Norwegian University of Science and Technology
Faculty of Information Technology and Electrical Engineering
Department of Electric Power Engineering

Stian Nessa

New Environmentally-friendly Insulation Gases

Pre-breakdown and Breakdown Mechanisms near Insulating Surfaces under Fast Voltage Impulses

Master's thesis in Energy and the Environment
Supervisor: Frank Mauseth
Co-supervisor: Hans Kristian Hygen Meyer
June 2022

NTNU
Norwegian University of Science and Technology

Stian Nessa

New Environmentally-friendly Insulation Gases

Pre-breakdown and Breakdown Mechanisms near Insulating Surfaces under Fast Voltage Impulses

Master's thesis in Energy and the Environment
Supervisor: Frank Mauseth
Co-supervisor: Hans Kristian Hygen Meyer
June 2022

Norwegian University of Science and Technology
Faculty of Information Technology and Electrical Engineering
Department of Electric Power Engineering

NTNU
Norwegian University of
Science and Technology

Abstract

With the current push for phasing out SF_6, new designs for high voltage equipment are needed to minimize the impact of the shift to more environmentally friendly insulating gases. To achieve this, a deeper understanding of electric discharges in alternative gases is required.

This thesis is a continuation of a previous project where a sudden increase in breakdown voltage was observed under particular conditions. The phenomenon occurs when a fast positive voltage impulse is applied across a rod-plane gap with a dielectric surface placed a small distance away from and parallel to the electrode. The work performed for this thesis investigates other aspects of this phenomenon, including how it is affected by the distance between the surface and electrode, and negative impulses.

Up-and-down testing was performed for varying geometries under positive impulses and for negative impulses to observe changes in breakdown voltage. High-speed imaging was performed to observe discharge behavior within the gap.

In addition to this investigation is a second investigation into a new strategy for surface charge removal. This strategy is based on evaporating a thin layer of carbon onto a surface to increase its conductivity slightly. This strategy was shown to be successful for impulse voltages in the previous project and is in this thesis being tested for AC. To investigate this, the test object was subjected to AC at an increasing voltage both with and without the dielectric surface. The breakdown voltages were recorded and compared to uncover potential decreases and an IR camera was used to uncover any excessive surface heating.

The up-and-down tests show that the breakdown voltage under fast positive voltage impulses is highly sensitive to the distance between the surface and the electrode. There is a significant increase in breakdown voltage at a distance of 20 mm, but with a much smaller increase when placed both closer or farther away. The tests also showed that the breakdown voltage increase is not present for negative voltage impulses. Additionally, the images captured using high-speed cameras showed that certain discharges are affected by the parallel surface. The breakdown tests and the thermal camera showed no significant negative effects caused by the evaporated carbon layer during AC application.

Sammendrag

Med det nåværende presset for å fase ut SF_6, er det nødvendig med nye design av høyspentutstyr for å minimere konsekvensene av overgangen til mer miljøvennlige isolasjonsgasser. For å oppnå dette kreves en dypere forståelse av elektriske utladninger i alternative gasser.

Denne avhandlingen er en videreføring av et tidligere prosjekt hvor det ble observert en uventet økning i gjennomslagsspenning under spesielle forhold. Fenomenet oppstår når en rask positiv spenningsimpuls (stigetid på 200 ns) påføres over et stang-plan gap med en dielektrisk overflate plassert kort avstand unna og parallelt med elektroden. Arbeidet som er utført for denne avhandlingen er en undersøkelse av andre aspekter ved dette fenomenet, som inkluderer hvordan det påvirkes av avstanden mellom overflate og elektrode, og negative impulser.

Opp-og-ned-testing ble utført for varierende geometrier for positive impulser og for negative impulser for å observere eventuelle endringer i gjennomslagsspenningen. Høyhastighetsbilder ble tatt for å observere utladningsatferd i gapet.

I tillegg til denne undersøkelsen ble det også gjennomført en undersøkelse av en ny strategi for fjerning av overflateladninger. Denne strategien er basert på å fordampe et tynt lag karbon på en overflate for å marginalt øke ledningsevnen. Denne strategien ble vist til å fungere for impulsspenninger i det tidligere prosjekt, og testes i denne oppgaven for vekselspenning. For å undersøke dette ble testobjektet utsatt for stegvis økende vekselspenning både med og uten den dielektriske overflaten. Gjennomslagsspenningene ble registrert og sammenlignet for å avdekke eventuelle reduksjoner, og et IR-kamera ble brukt for å avdekke overdreven overflateoppvarming.

Opp-og-ned-testene viser at gjennomslagsspenningen under raske positive impulser er svært følsom for avstanden mellom overflaten og elektroden. Med stor økning i sammenbruddsspenning med en avstand på 20 mm, men en mye mindre økning både nærmere eller lengre unna. Testene viste også at gjennomslagsspenningsøkningen ikke er tilstede for negative spenningsimpulser. I tillegg viste bildene tatt med høyhastighetskameraene at visse utladninger påvirkes av den parallelle overflaten. Nedbrytningstestene og termisk kamera viste ingen signifikante negative effekter forårsaket av det pådampede karbonlaget under påføring av vekselspennings.

Preface

I would like to thank my supervisor Frank Mauseth and my co-supervisor Hans Kristian Hygen Meyer for their time, help, and expertise. I would also like to thank Robert Marskar and Dag Linhjell from Sintef for their input on both the theoretical and practical parts of my work.

My laboratory work would not have been possible without Morten Flå, Dominik Häger, and the service lab crew who has helped me immensely with all my equipment needs.

Finally I would like to thank my laboratory cohabitants Fredrik Leonardie Bratland and Fanny Skirbekk for their help with my experiments, and all my fellow students in room F452 for the good times.

Stian Nessa
Trondheim, June 2022

Contents

1 Introduction

With the ever-increasing focus on electrification and climate action, the pressure is building rapidly for not only the production of renewable energy but also for its safe, reliable, and sustainable transmission and distribution. High voltage equipment requires more space efficient and cost-saving innovations to meet the energy and environmental requirements of the near future.

Traditionally, SF_6 has been the most widely used insulating gas in gas-insulated systems (GIS) due to its excellent dielectric- and chemical properties. With its high dielectric strength and electron negativity, GIS using SF_6 can be significantly smaller and more compact than air-insulated systems. However, the biggest challenge with SF_6 is its huge environmental impact. SF_6 is considered the worst greenhouse gas that has been classified with a greenhouse potential (GWP) of over 23 000.

This has put a lot of pressure on the industry to investigate new alternative gases and technologies to eliminate the use of SF_6, and requires direct testing of alternative gases and a deeper understanding of how discharges may interact with dielectric surfaces. Further research is required to be able to predict and simulate how these discharges will behave and thus be able to simplify design processes.

1.1 Scope of work

This thesis investigates a particular phenomena that appears under particular circumstances, aiming to further our understanding of discharges and breakdowns during fast voltage impulses. This phenomenon may appear when a surface is placed parallel to an air gap and a fast voltage impulse, with a rise time of a few hundred nanoseconds, is applied across the gap. This phenomenon was previously shown to increase the breakdown voltage of the air gap, and this thesis continues the investigation into other aspects of the phenomena. This thesis only focuses on atmospheric air.

In parallel to this research, further testing of a method of surface charge removal was performed. The method was developed because of a need to more easily remove surface charges from a surface. This need arose due to tests from [1]

showing that surface charges significantly affected the tests. The results from this test is shown in Appendix A. This method was first utilized and tested in the precursor project [1] to this thesis, where it was shown to be effective at removing surface charges without affecting lightning impulse breakdown voltages. The results from this test is also shown in Appendix A. Further verification is performed to uncover possible applications and limitations. In this thesis, the focus is on AC application.

Due to the highly stochastic nature of discharges, acquiring good data and high-speed images is challenging and time-consuming. For some parts of this thesis, this may limit the number of relevant images available and gives some outliers within the data.

1.2 Research questions

To focus the investigation into the two research areas mentioned above, four research questions were composed, with three pertaining to the fast voltage impulse phenomena and one pertaining to the evaporated carbon layer.

The research questions for this thesis are

1. How does the distance from a parallel surface to an electrode affect the electric field distortion and breakdown voltage for fast positive voltage impulses?
2. How does a parallel surface affect the breakdown voltage for fast negative voltage impulses?
3. How does a parallel surface affect discharges in an air gap during fast voltage impulses?
4. Does an evaporated carbon layer applied to a parallel surface negatively affect AC breakdown voltage and/or cause excessive heating?

2 | Theory

This chapter will summarize some critical theory within the realm of discharge physics in air that will be important later in this thesis. It is assumed that the reader has some previous knowledge about electric discharges and some particle physics.

2.1 Streamer discharges

Streamers are discharge phenomena that consist of a cold plasma filament with a highly charged layer surrounding it, as represented in Figure 2.1 [2]. Depending on voltage polarity, the ionized layer is made up of either positive ions or electrons. Because of the concentrated charge density caused by the curvature of the front of the streamer discharge, a highly localized enhanced electric field is created at its head . This enhanced field at the head may then facilitate further discharges by ionization and further extend the streamer channel even in background fields lower than the breakdown field of air. As the streamer moves further into the medium, the high field enhancement moves with the streamer head, and the tail of the streamer will not be able to emit light. This means that even though many images and figures depict streamers as long streaks of light, they are often long-exposure photographs or simplifications. The light emissions, the electric field, the electron density, and the charge density of a streamer discharge is shown in Figure 2.2.

This runaway ionization process is highly stochastic by nature and especially dependent on the non-ionized medium it grows into. In general for a streamer to grow, the number of free electrons created by ionization must exceed the number of electron being reattached to positive ions [2]. Both these processes are affected by e.g. gas pressure, electronegativity/electropositivity, and applied voltage.

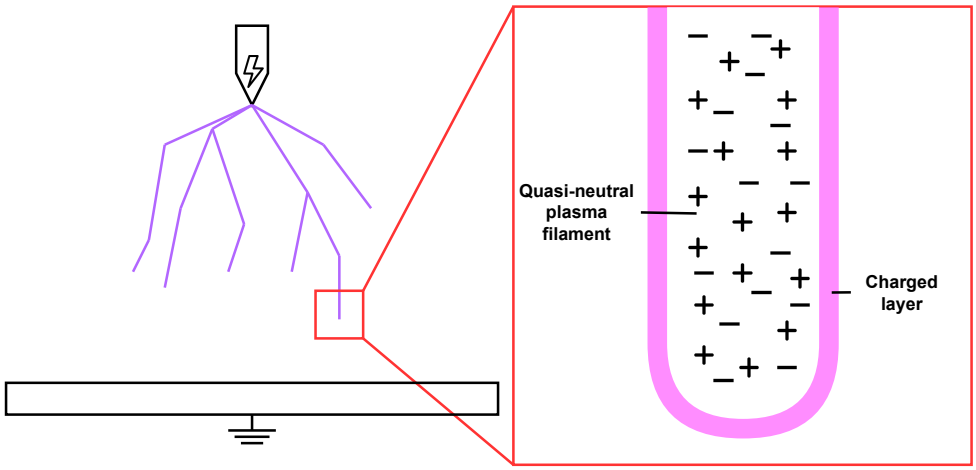

Figure 2.1: A conceptual figure of the cold plasma filament of a streamer discharge.

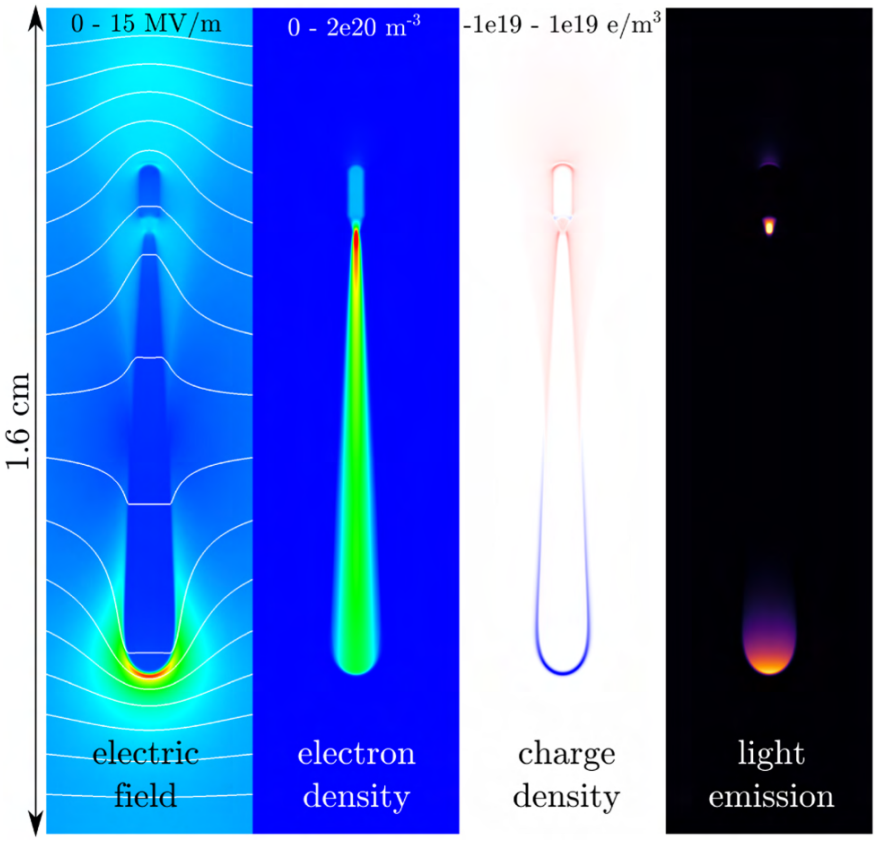

Figure 2.2: A plot of a streamer discharge showing the electric field distribution, the electron density, the charge density, and light emission [2].

2.1.1 Negative streamer discharges

Negative streamer discharges are anode-directed streamer discharges and therefore move against the electric field in the direction of the electron drift [3]. The charge layer consists of electrons [2].

The most important ionization process for negative streamer discharges is impact ionization [4]. Impact ionization occurs when a free electron is accelerated in an electric field and collides with a neutral atom. If the electron has sufficient energy, the impact between the accelerated electron and the bound electron may transfer enough energy to free the previously bound electron. A simple representation of this process is shown in Figure 2.3 and Figure 2.4. This process leads to electron multiplication, and these secondary electrons are then accelerated and may go on to free more electrons.

As this process continues, the secondary electrons become the moving front of the streamer discharge, while the positive ions left behind form the filament. Due to the higher drift velocity, electrons in the charged layer of negative streamer discharges will drift farther apart than positive ions in positive streamer discharges [2]. This decreases the field enhancement of negative streamer discharges in comparison to positive streamer discharges which will be discussed in subsection 2.1.2.

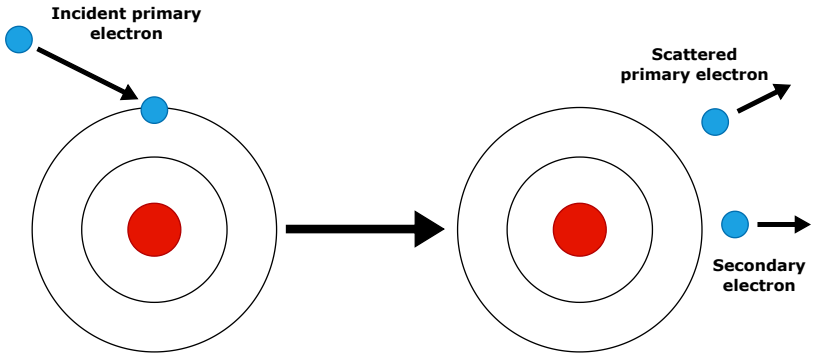

Figure 2.3: A conceptual figure showing impact ionization of an atom [5].

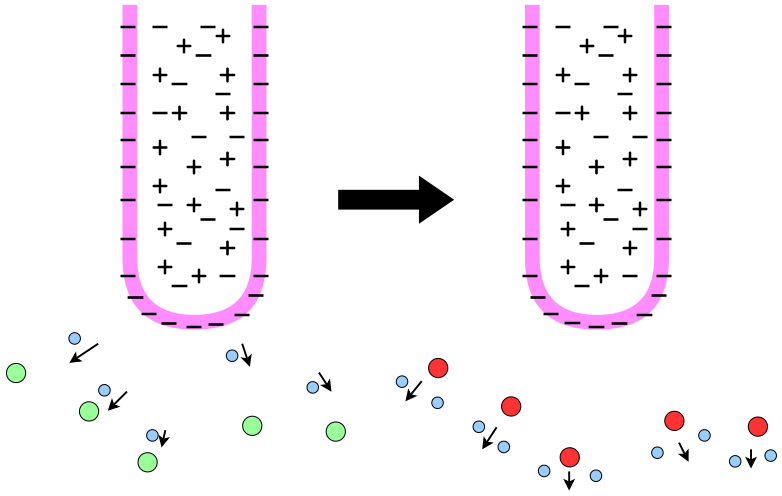

Figure 2.4: A conceptual figure showing how negative streamer discharges propagate using impact ionization with neutral atoms in green, positive ions in red, and electrons in blue.

2.1.2 Positive streamer discharges

In contrast to negative streamer discharges, positive streamer discharges are cathode-directed, which means they grow in the direction of the electric field. The streamer discharge front layer consists of positive ions, which move more than an order of magnitude slower than electrons. This means that the front does not move because of ion movement but because of ionization in front of the discharge.

Positive streamer discharges are initiated by an initial electron avalanche towards the anode, which leaves behind a positive space charge. As more avalanches occur, new avalanches may be initiated by photoionization and the strong fields close to the positive space charge.

The primary ionization mechanism for positive streamers is also impact ionization, but positive streamer discharges also require a source of free electrons [2]. The free electrons needed for positive streamer propagation in air are mainly produced via photoionization.

Photoionization is when high-energy photons, typically in the UV and x-ray range, are emitted from the streamer head into the surrounding non-ionized medium. As these photons hit neutral atoms, the energy transferred to the orbiting electron may be enough to detach from its atom, thereby creating an electron-ion pair. The free electron may then be accelerated towards the streamer discharges' positive space charge, leaving behind its positive ion. As this process and the resulting avalanches occur as a thick cloud, the ions are left behind to create the aforementioned positive space charge [2].

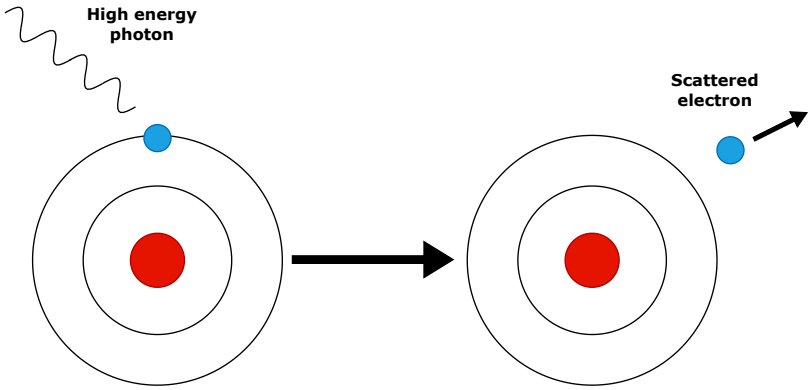

Figure 2.5: A conceptual figure showing photon ionization of an atom

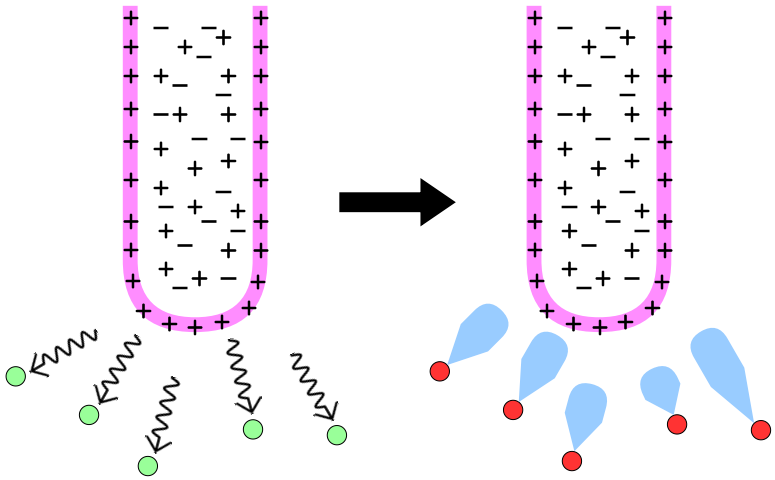

Figure 2.6: A conceptual figure showing how positive streamer discharges propagate using photo ionization creating electron avalanches with neutral atoms in green, positive ions in red, and electron avalanches in blue.

2.2 Leader discharges

In contrast to a streamer discharges, leader discharges are hot plasma channels that may form as a consequence of heating inside cold discharges, such as streamer channels. Leader discharges are often formed due to excessive heating and gas expansion inside streamers or corona until around 1500-2000 K when gas into this hot plasma and the conductivity of the filament increases sharply [6]. Because of the high plasma temperature, leader discharges are much brighter than streamers due to thermal radiation and increased ionization activity. This increase in conductivity and temperature facilitates further ionization and streamers at its front, which causes the leader to continue to grow [2]. Due to

the much higher conductivity, the potential of the electrode may be transferred to the leader discharge, making the leader discharge act as an extension of the electrode [7].

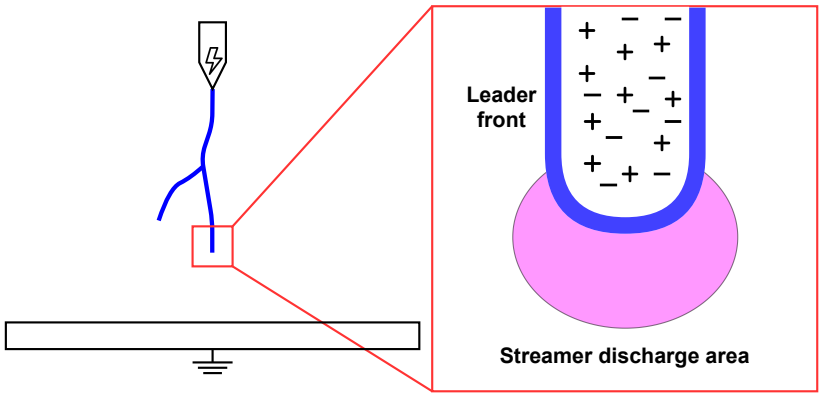

Figure 2.7: A conceptual figure of the plasma filament of a leader discharge, showing that the leader propagates by streamer discharges at its head.

2.3 Surface charges

In high voltage applications, dielectric interfaces are critical as they may significantly influence fields and discharges [8]. One an interface the electric fields is through surface charges, which are free charges in the air that may accumulate at an interface between for example a gas and a dielectric solid when an electric field is applied. These surface charges may significantly distort the tangential electric field, possibly affecting discharges [9].

However, for surface charges to accumulate, free charges must be available near the surface. One significant source of free charges are electric discharges that propagate close to surfaces [9]. This makes surface charges very complex, and simplification must be made to be able to predict them.

Based on Gauss' law, the charges on an interface

$$\varepsilon_{sol} E_{n,sol} - E_{n,air} = \sigma_s \tag{2.1}$$

where ε_{sol} is the permittivity of the solid, $E_{n,sol}$ and $E_{n,air}$ is the normal electric field in the solid and air respectively, and σ_s is the surface charge [8].

As the surface charges depend on many variables, the simplest cases to consider are when there are no surface charges or when the surface charges cancel out the normal component of the field strength [9]. This last condition is called surface saturation and may be expressed as

$$E_{n,air} = 0 \tag{2.2}$$

Inserting this condition into Equation 2.1, the saturation charge is then

$$\varepsilon_{sol} E_{n,sol} = \sigma_{sat} \tag{2.3}$$

where σ_{sat} is the saturation charge. A conceptual figure showing the fields in these two extremal cases is shown in Figure 2.8. This approximation is good for calculating stationary fields; however, surface charges become more complicated when discharges are involved. Discharges, especially leader discharges, may significantly alter the initial electric field distribution, pushing the surface charges beyond the originally calculated surface charge.

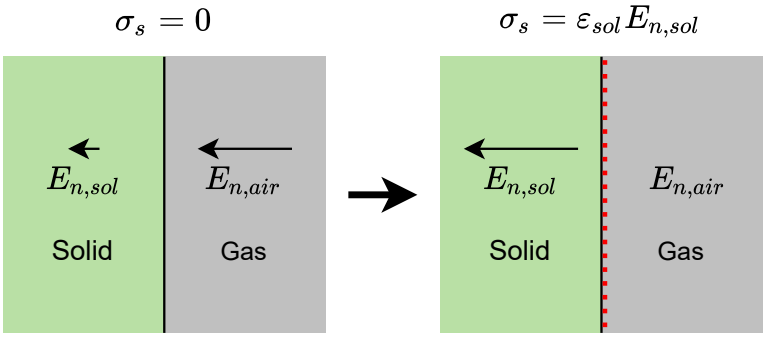

Figure 2.8: The normal electric fields at the interface between a gas and a dielectric solid both without surface charges and at surface charge saturation.

3 | Experimental setups and procedures

This chapter will introduce the experimental setups and procedures that was used during the thesis work and is split into three parts. The first section introduces the complete test object used throughout all experiments. The second and third sections presents setups and equipment specific to fast voltage impulse testing and AC testing respectively.

3.1 Test object

For this thesis, the surface used to investigate was chosen to be a polycarbonate sheet with the dimensions shown in Figure 3.1, which is supported by a bracket that provides stability. The polycarbonate sheet is covered in a thin layer of carbon applied using carbon evaporation. In short, the polycarbonate is placed in a vacuum dome together with two carbon electrodes. These carbon electrodes have a high contact resistance and are heated using current until the carbon begins to evaporate. The evaporated carbon expands into the vacuum and leaves a layer of carbon believed to be only a few atoms thick. This process is described in detail in the preceding project for this thesis [1].

This layer was shown not to affect impulse testing in [1], and the relevant test results are shown in Appendix A.

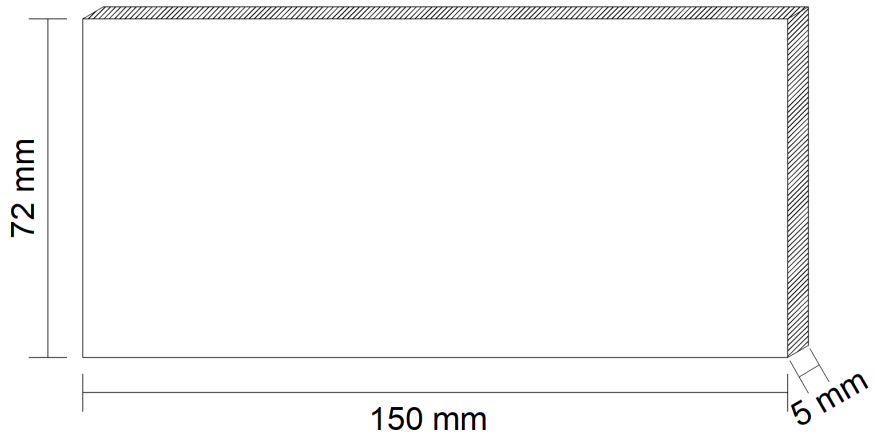

Figure 3.1: The polycarbonate sheet with a thin carbon layer used as a surface during experiments.

Experiments were performed using two different electrodes based on application. One electrode, shown in Figure 3.2, is used to simulate real-world geometry and creates a homogeneous field. The other electrode, shown in Figure 3.3, is a needle electrode designed to create an inhomogeneous field and is used produce discharges more easily.

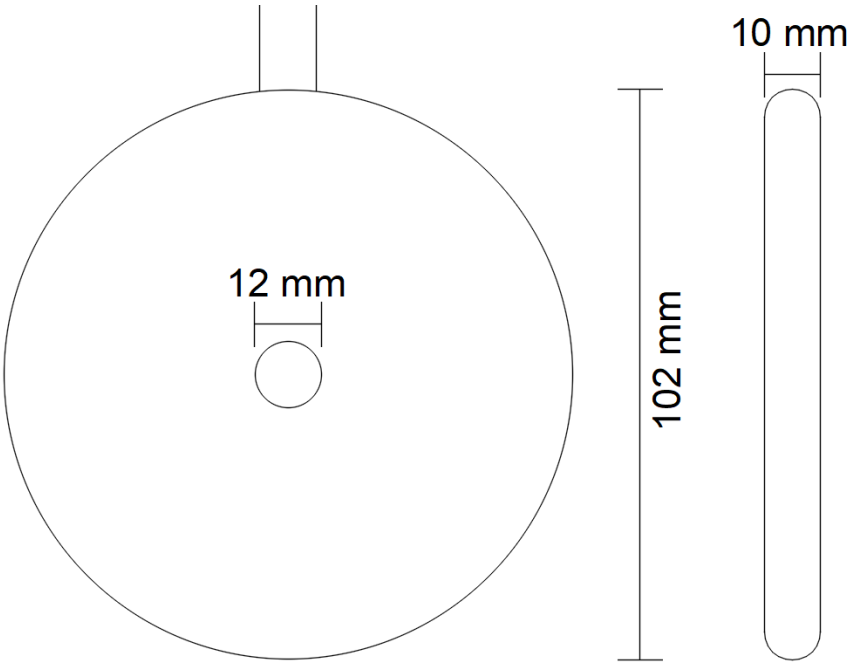

Figure 3.2: Dimensions for the round electrode used to create homogeneous fields.

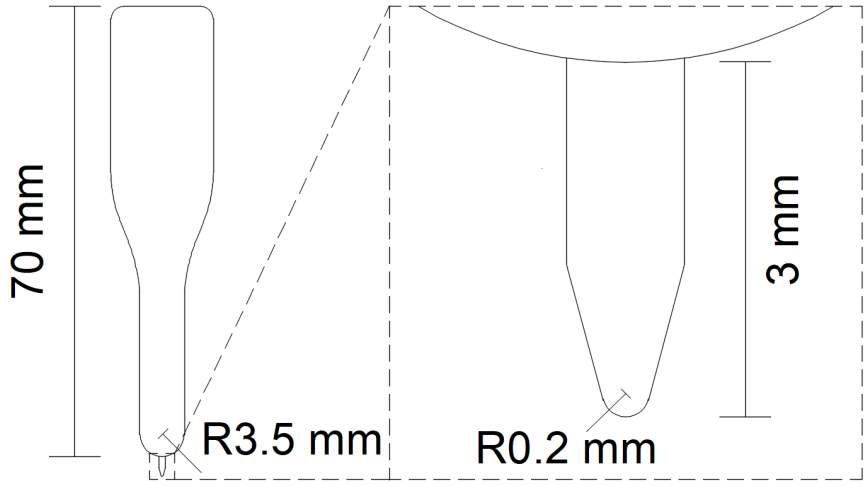

Figure 3.3: Dimensions for the needle electrode used to create inhomogeneous fields.

For this thesis, the height of the electrode is fixed at 40 mm; however, the distance between the parallel surface and the electrode is variable. This means that for further experiments and discussions, the distance always refers to this distance between the surface and electrode, as represented in Figure 3.4.

A 3D representation of the complete test object is shown in Figure 3.5.

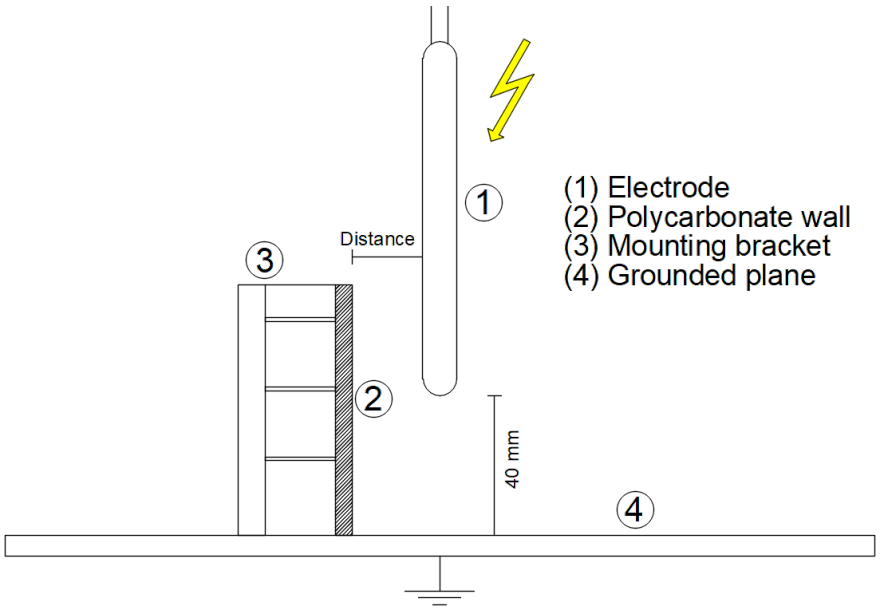

Figure 3.4: A 2D representation of the test object with the variable distance of the surface shown [1].

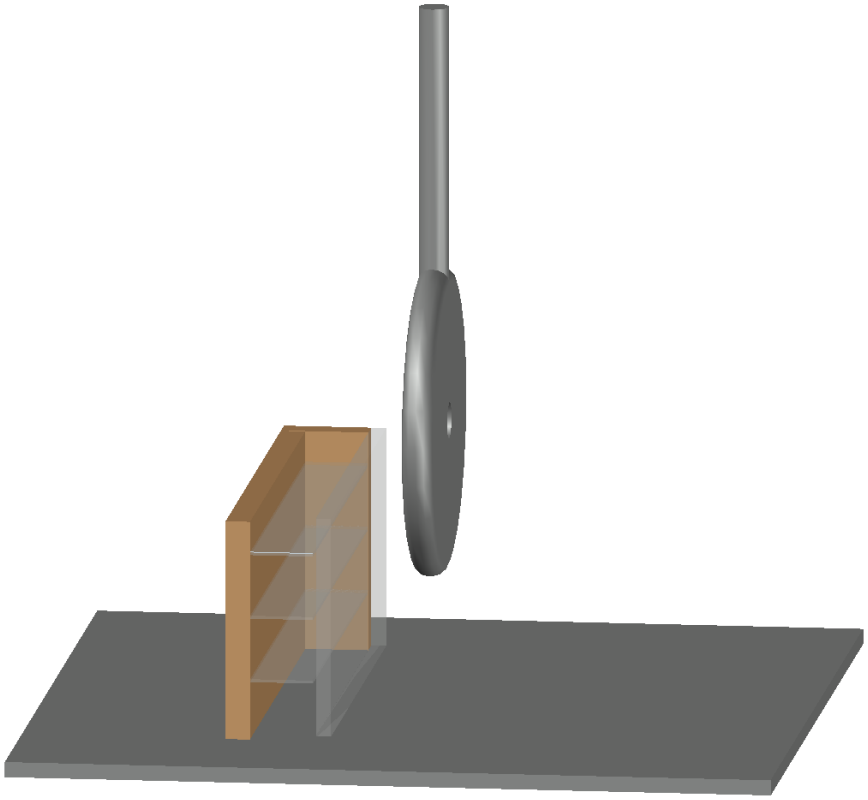

Figure 3.5: A 3D representation of the test object used with one of the two electrodes.

3.2 Voltage impulse testing

This section gives an overview of the setup and methodology used during all lightning impulse experiments performed during this thesis. This includes experimental setup, an introduction to specific components of interest, and a statistical method used during the experiments.

3.2.1 Experimental setup

The test setup consists of the test object, the 1.2 MV impulse generator with its accompanying control systems, and an oscilloscope connected to a capacitive- and a resistive voltage divider. There is also a current limiting resistor between the front capacitor and the test object. A schematic overview of the setup is presented in Figure 3.6.

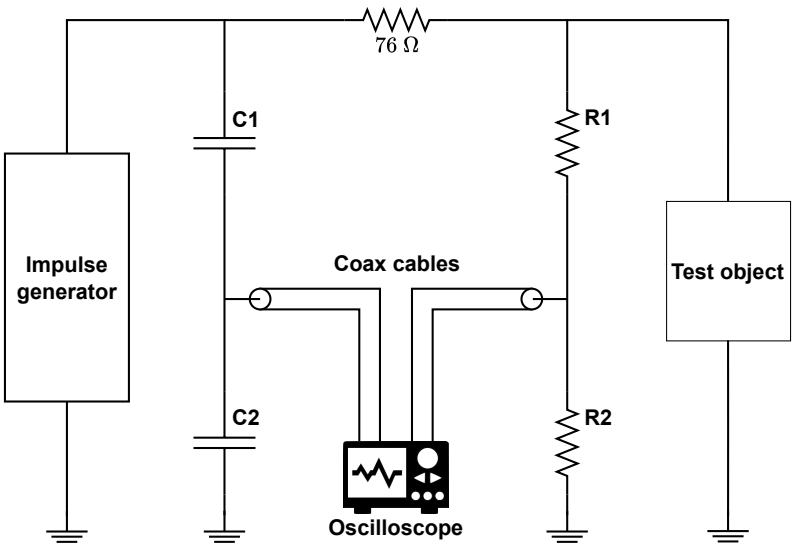

Figure 3.6: Schematic drawing of the test setup used for fast voltage impulse testing.

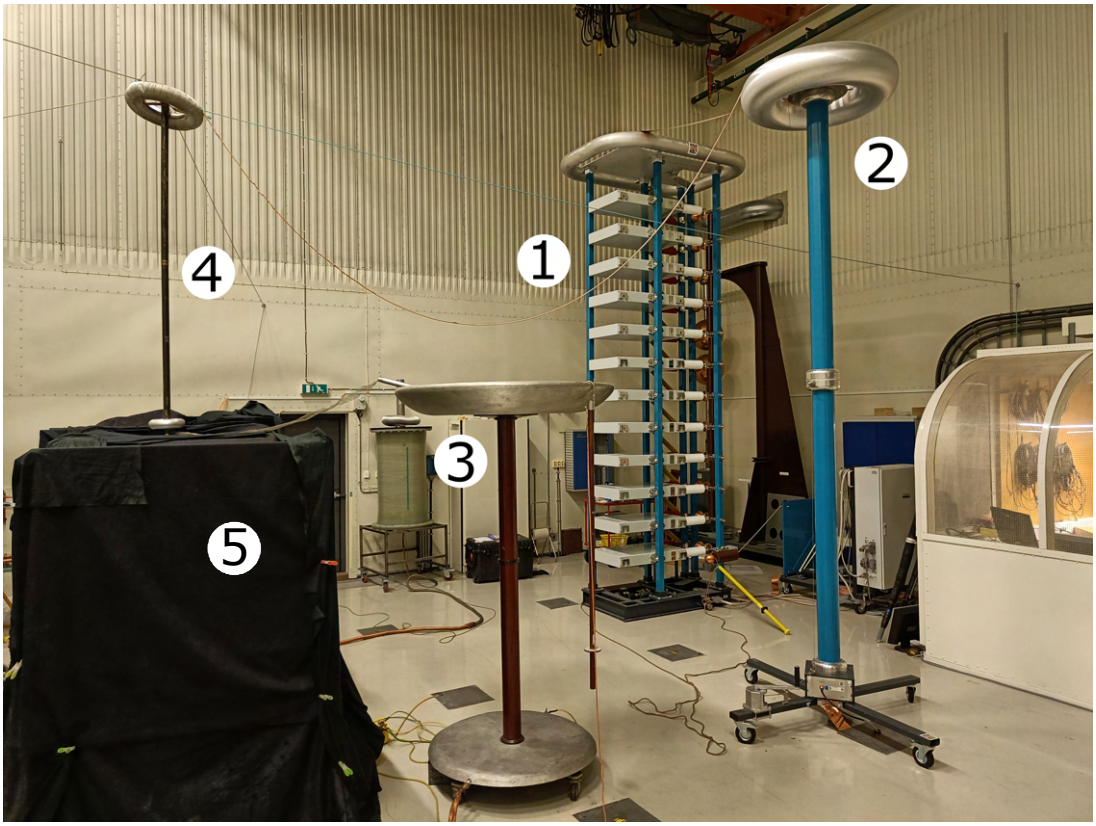

Figure 3.7: (1) Impulse generator (2) Capacitive voltage divider (3) Resistive voltage divider (4) High voltage connection to pressure vessel with 76 Ω resistor (5) Dark tent housing the test object, PMT, and cameras.

3.2.2 Voltage supplied by the impulse generator

For this thesis, the impulse generator used was a 12 capacitor Marx generator with a maximum voltage of 1.2 MV (100 kV per capacitor). Because of a minimum voltage per capacitor, a single capacitor was used as all voltages used during experiments were under 100 kV. Initially, the only voltage measurement performed was the capacitive divider measurement. This appeared to give voltage impulses with a rise time of about 500 ns and a slight voltage overshoot. However, a new voltage rise time was discovered after the resistive measurement was added.

The resistive measurement had the benefit of being connected almost directly to the electrode. This measurement showed a much faster rise time than the one measured capacitively. The voltage peak was also measured to be slightly higher.

A short investigation using a North star PVM-100 voltage probe was performed to determine the actual voltage experienced at the test object. The probe was connected directly to the electrode, and several tests were performed both with and without the resistive divider at different voltages. It was determined that

the resistive divider influenced the voltage at the electrode when connected, but it also accurately measured the voltage when connected.

The investigation determined that when the resistive divider was connected, the voltage measured was used as-is. However, with only the capacitive divider connected, a factor of 1.155 was determined to be the ratio between the charging voltage and the peak voltage. This factor was determined to be linear for the relevant voltage range.

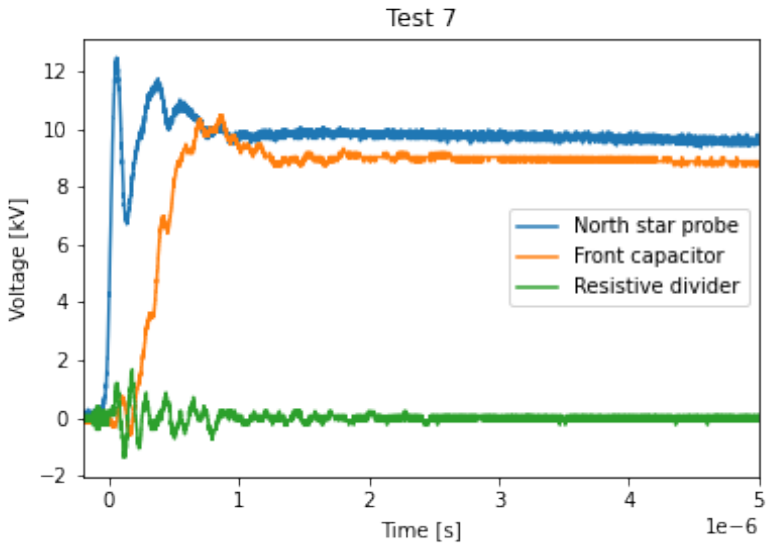

Figure 3.8: Voltage measurement with only the capacitive voltage divider connected measured using a North star PVM-100 voltage probe.

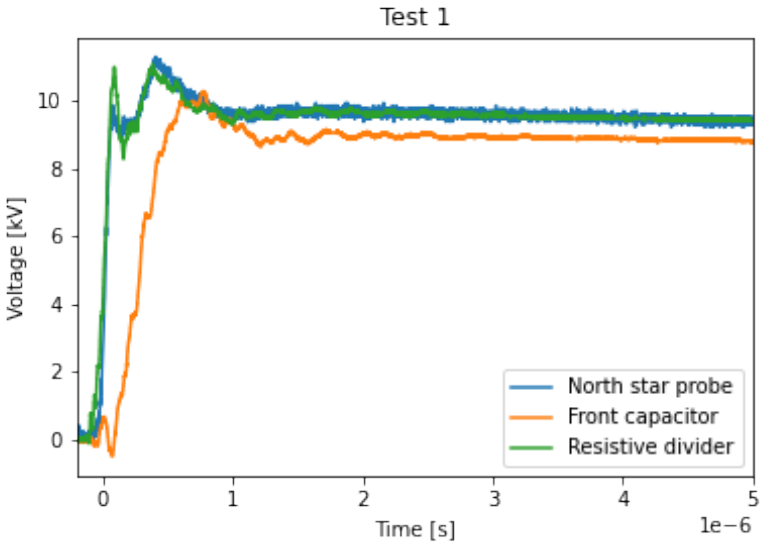

Figure 3.9: Voltage measurement with both voltage dividers connected measured using a North star PVM-100 voltage probe.

3.2.3 Photomultiplier tube

A photomultiplier tube, or PMT, is a device used to detect photons and significantly amplify the resulting output signal. The PMT does this by having the photon excite a photocathode at the front of the tube, which releases an electron when hit by a photon. The electron is then accelerated using multiple dynodes, with every subsequent dynode having an increased voltage into the tube. As the electrons hit these dynodes, additional electrons are excited and will be accelerated by the field further into the tube. At the end of the tube is the anode that will output a small negative voltage when hit by the electrons. A conceptual representation of this process is shown in Figure 3.10, and a plot of the PMT signal on an oscilloscope is presented in Figure 3.11.

For these experiments, the PMT is used to confirm the presence of streamer discharges and for timing adjustments for high-speed imaging.

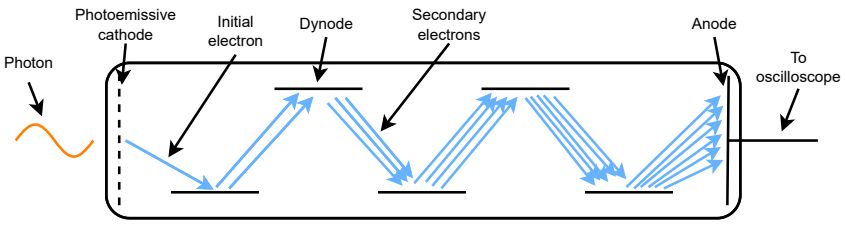

Figure 3.10: A conceptual schematic of a PMT showing electron multiplication.

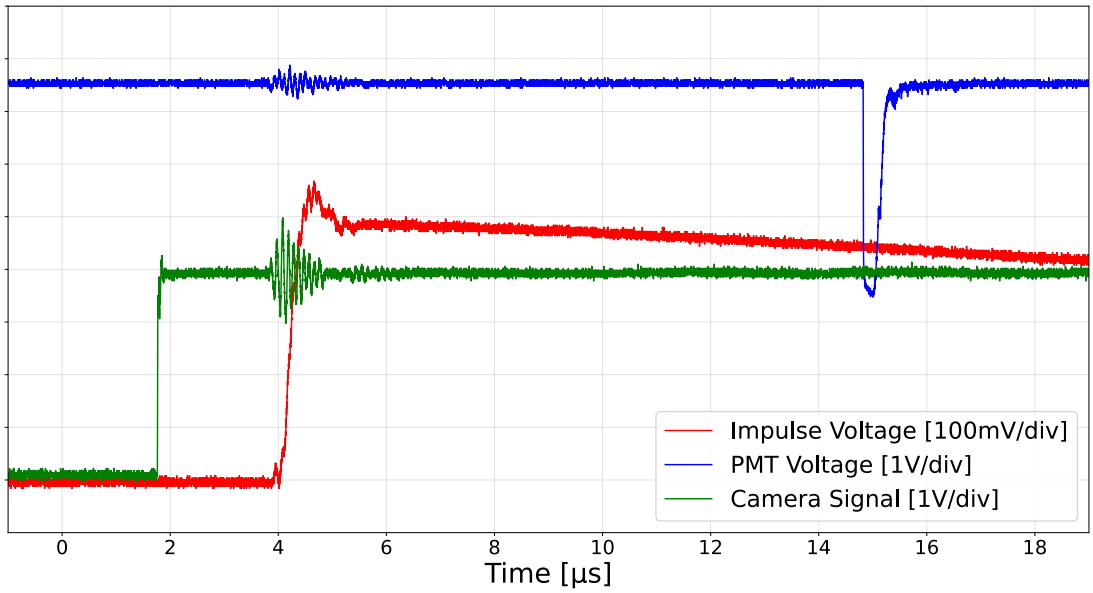

Figure 3.11: An example of a signal from the PMT caused by light from streamer discharges.

3.2.4 High-speed imaging

As streamer- and leader discharges are very fast phenomena, high speed- and highly light-sensitive cameras are required to capture images with a high enough resolution. Two separate cameras are used depending on the application, with one having a better light intensifier and the other able to capture multiple frames. The two cameras are presented below.

Lambert HiCam

The Lambert HiCam is a high-speed camera with two light intensifiers giving very high-resolution images in low-light environments. The HiCam is used as a "long exposure" single image camera for this thesis. An exposure time of 200 μs captures a single frame containing the accumulated light of all discharges.

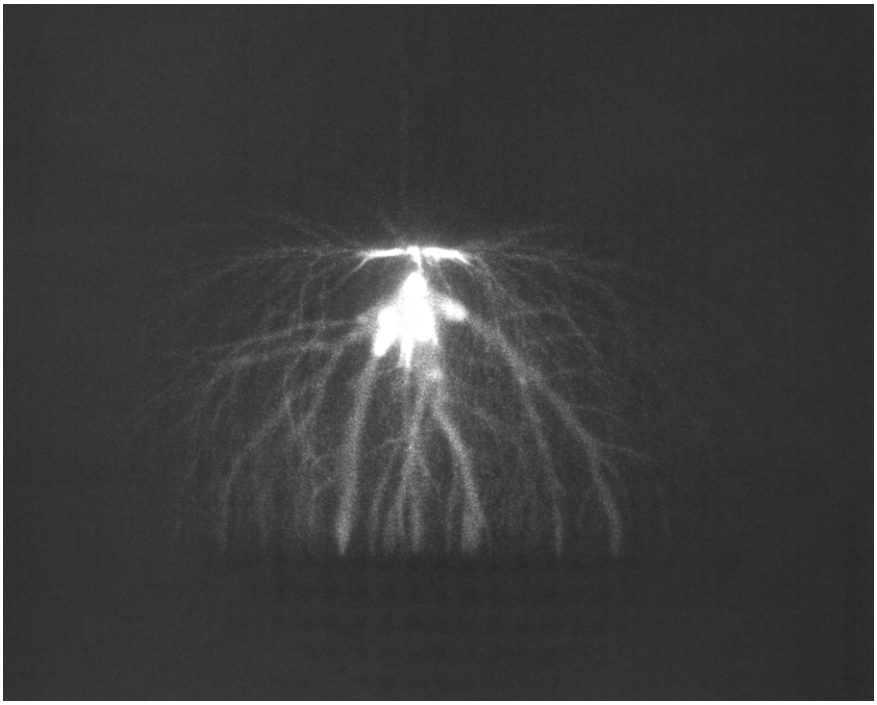

Figure 3.12: An example image captured using the Lambert HiCam.

SIMX16

SIMX16 is a high-speed, light-intensified camera used in applications demanding high framerates and resolution. Depending on the configuration, the camera can capture 16 or 8 consecutive images in a small time frame, with a minimum exposure time of 3 ns per image and the possibility of 2 ns interframing. Interframing is when a new frame exposure is started before the previous frame is finished. This gives a minimum time between frames of only 1 ns, or 1 billion frames per second. The timings and exposures are entirely configurable by the user and may be done on a frame-by-frame basis.

For this thesis, the first frame was typically reserved for use as a long exposure frame relative to the other frames. It will either capture light across all other frames or everything leading up to the second frame, depending on what discharge is being captured.

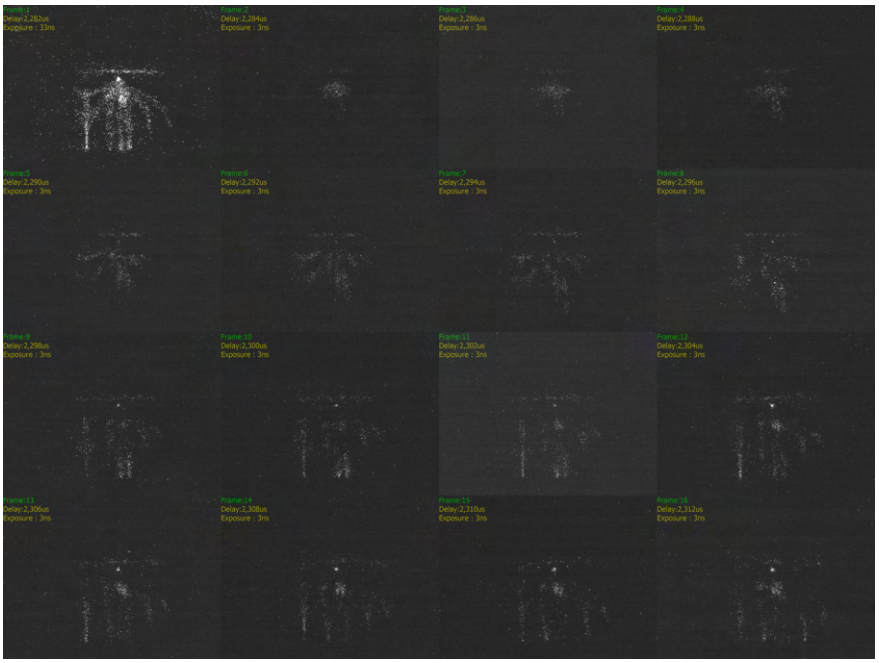

Figure 3.13: An example of a 16 image series captured using the SIMX16 camera.

3.2.5 Up-and-down method

The up-and-down method is an algorithmic statistical method of estimating a test object's 50% breakdown voltage using relatively few lightning impulses, with the minimum being 20 [10]. A flowchart of the algorithm is presented in Figure 3.15.

To perform an up-and-down test, ΔU must first be chosen for the test and should be approximately equal to the standard deviation of the assumed normally distributed breakdown voltage. The next step is estimating the lowest voltage where a breakdown may occur, which is difficult to estimate and will therefore be based on an educated guess.

Perform a lightning impulse at a voltage slightly lower than the estimated lowest breakdown voltage, and increase the voltage by ΔU if a breakdown did not occur. Continue performing lightning impulses and increasing the voltage until the first breakdown occurs. This first breakdown is considered the first result of the test and all subsequent impulses are recorded.

After the first breakdown, a predetermined number of impulses are now performed in series. After each impulse, the voltage is either increased or decreased depending on the result of the previous impulse. In the case of a breakdown, the

voltage is decreased by ΔU, and the voltage is increased by ΔU if the test object withstands the impulse. When the predetermined number of impulses are performed, the results are analyzed and the 50% breakdown voltage is calculated. An example of a generic up-and-down test is presented in Figure 3.14.

The 50% breakdown voltage may be calculated using the equation

$$U_{50\%} = U_0 + \Delta U \left(\frac{A}{k} - \frac{1}{2} \right) \tag{3.1}$$

where $A = \Sigma_{i=1}^{r} i k_i$ (k_i is the number of breakdowns that occurred at each voltage step i up from U_0) and k is the total number of breakdowns that occurred [11, 12].

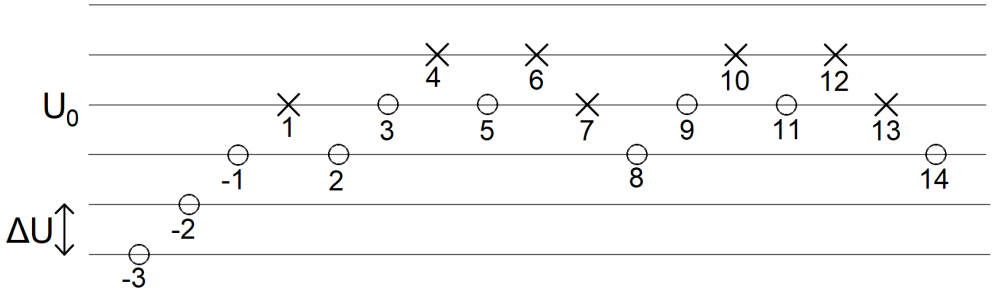

Figure 3.14: General example of an up-and-down test. The first recorded result is at first breakdown, where negative numbers signify initial impulses. X = Breakdown, O = Withstand, ΔU = Change in voltage between shots, U_0 = Lowest voltage where a breakdown occurred.

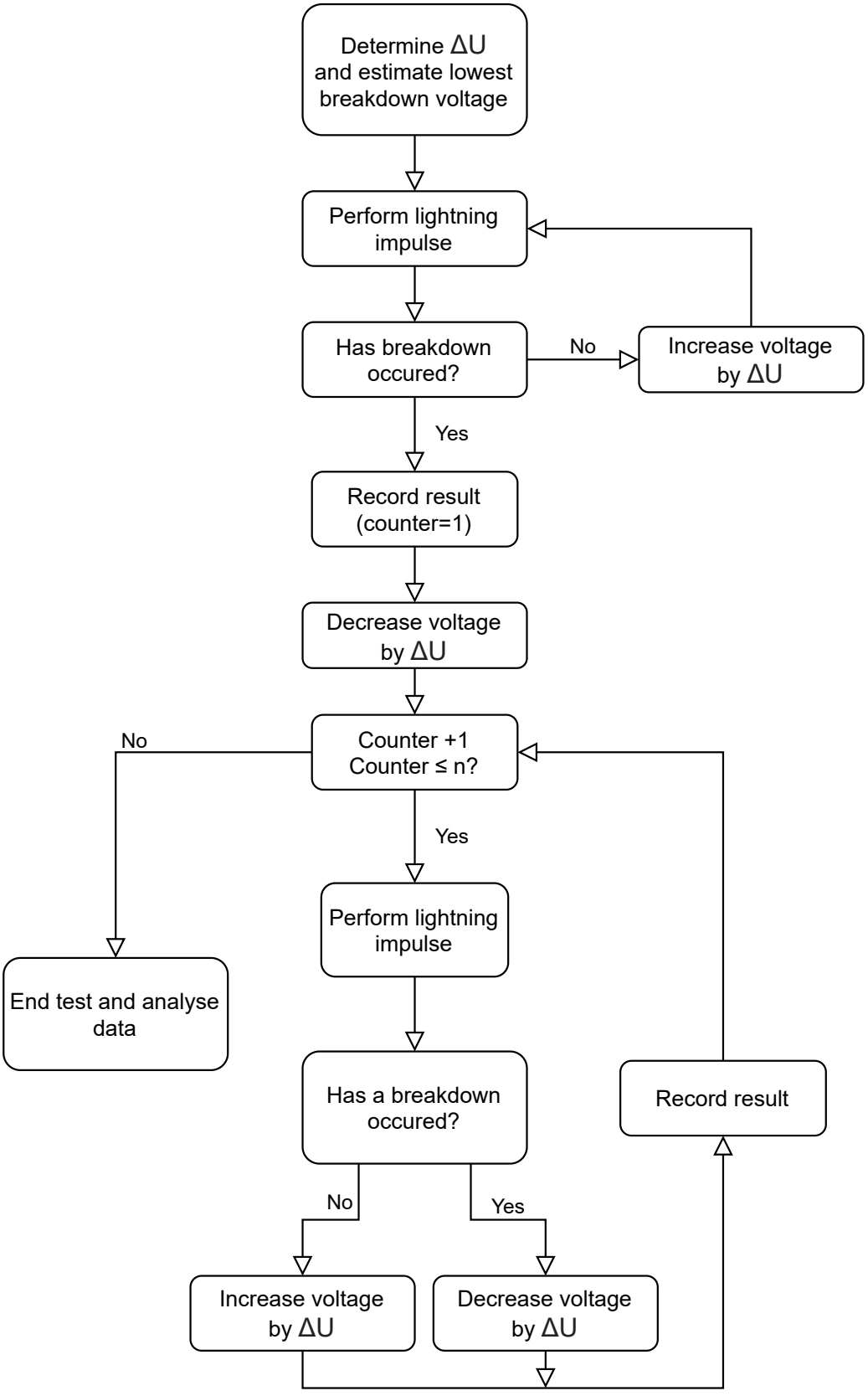

Figure 3.15: Algorithm for performing the up-and-down method [1].

3.3 AC testing

In order to be valid for testing purposes, the surface charge removal strategy of using evaporated carbon must not exhibit any negative effects during testing. In previous testing, the carbon layer was shown to be appropriate for voltage impulse testing [1]. To further understand the impact of the evaporated carbon layer, the surface is subjected to AC voltages to uncover any negative effects. The two main topics of concern are breakdown voltage and excess surface heating. Both measurements are performed in parallel during each test.

3.3.1 Experimental setup

The test setup for testing AC is shown in Figure 3.16. The variable high voltage is supplied by a variac on the low voltage side of a high voltage transformer. Voltage measurements are performed using a capacitive voltage divider connected to an oscilloscope on the high voltage side and a voltmeter connected across the terminals of the variac. Finally, the test object is connected to the transformer through a current limiting water resistor.

The thermal camera is set up on a tripod pointed at the test object and connected to a PC through USB to remotely monitor the temperature.

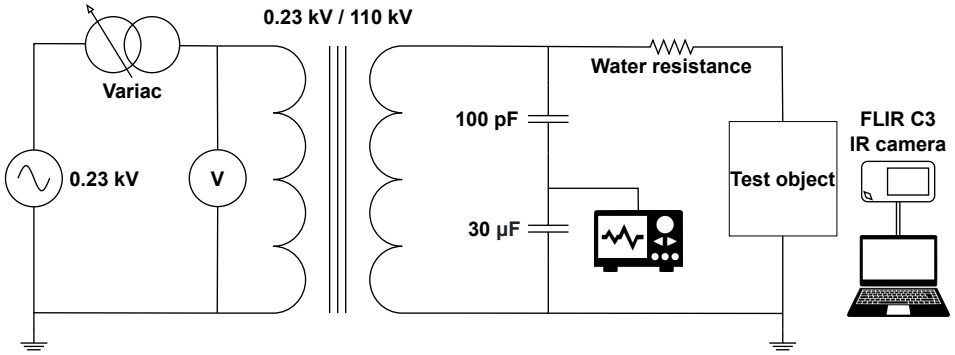

Figure 3.16: Schematic drawing of the test setup for AC testing of carbon layer.

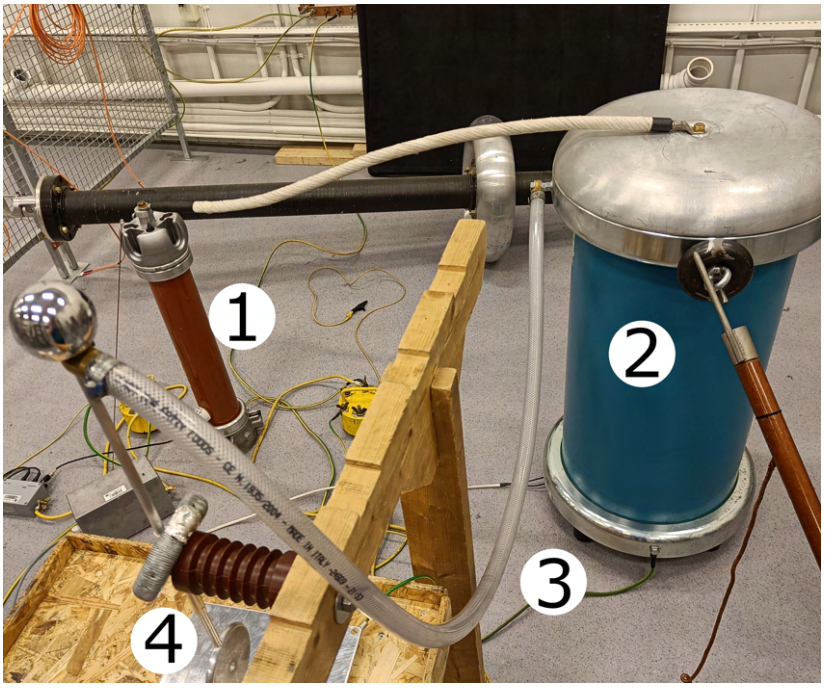

Figure 3.17: (1) Capacitive voltage divider (2) High voltage transformer (0.23/110 kV) (3) Water resistance (4) Test object.

3.3.2 Breakdown voltage

To investigate any potential problems with breakdown voltages during AC operation, the voltage is slowly increased until breakdown occurs, and this voltage is used as an initial estimate.

The voltage is then increased to 5 kV lower than the estimate found during the initial test and is kept at this voltage level for five minutes. If a breakdown does not occur during these five minutes, the voltage is then increased by 1 kV every minute until a breakdown occurs. The procedure is continued until breakdown occurs, and the procedure is completed five times to acquire an estimated breakdown voltage. This test is performed with and without the polycarbonate surface to uncover any significant change in breakdown voltage.

3.3.3 Surface heating

A FLIR C3 thermal camera is used to investigate potential heating issues caused by ohmic losses in the carbon layer. During the test described above, the thermal camera continuously monitors the polycarbonate's surface temperature. The camera is placed on a tripod and pointed at the test object from 2 meters away. The view of the test object from the camera is shown in Figure 3.18.

Figure 3.18: An image of the test setup captured using the FLIR C3 camera with the test setup shown in the middle of the frame.

4 | Electrostatic simulations

This chapter will present the model used for the electrostatic simulation performed using the commercial software Comsol multiphysics. Comsol is FEM (Finite element modeling) software used for multiphysics applications. For this thesis, the modeling was limited to stationary electrostatics.

4.1 Geometry and mesh

The geometry created in Comsol is presented in Figure 4.1 and consists of three main components. These include the gas volume represented by a surrounding rectangle, the surface and support bracket, and the electrode. As the electric potential is only interesting as a boundary condition, the electrode volume is cut out and not included in the model. To approximate this model to the real 3D space, the 2D model has an out-of-plane thickness.

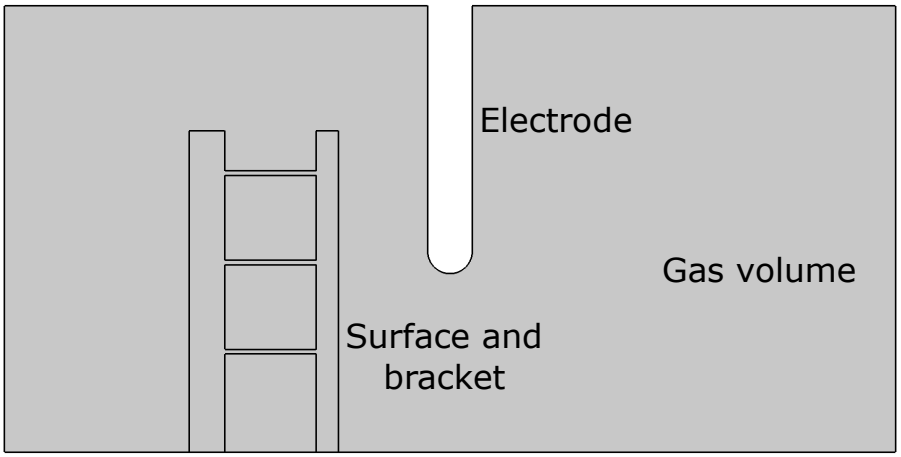

Figure 4.1: A 2D representation of the test object used as geometry for electrostatic simulations.

Comsol automatically creates the mesh used for the simulations, with the only user input being desired resolution. The mesh is shown in Figure 4.2.

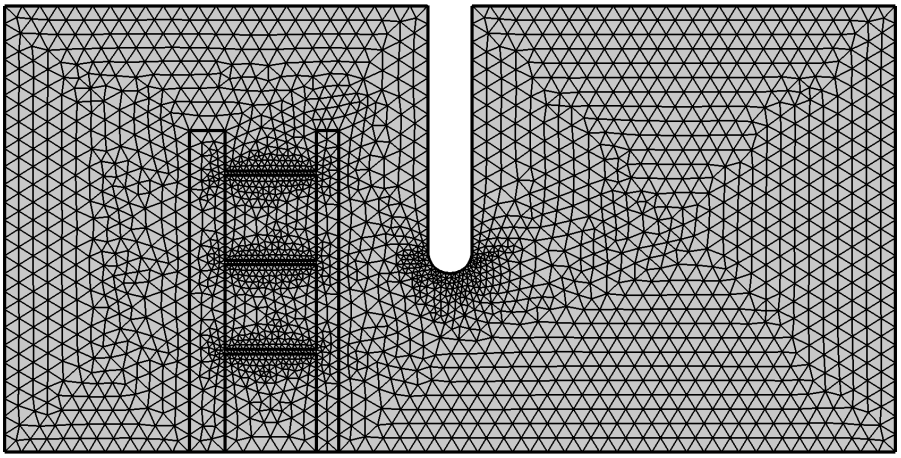

Figure 4.2: Mesh automatically created by Comsol based on the geometry with the resolution set to extra fine.

4.2 Electrostatics

To perform the field simulations, the following boundary conditions were applied to the model: An electric potential of 50 kV is applied to the boundary of the electrode, ground potential is applied to the bottom boundary of the air volume, and the zero charge condition is applied to the rest of the edges of the air volume.

The final boundary condition applied is surface charge density on the entire surface and bracket. This is based on the conditions presented in section 2.3. For simulations of the initial conditions without surface charges, this boundary condition is set to zero, while for simulations of saturation charge, the surface charge density is set to be minus the normal displacement field strength on the air side of the surface.

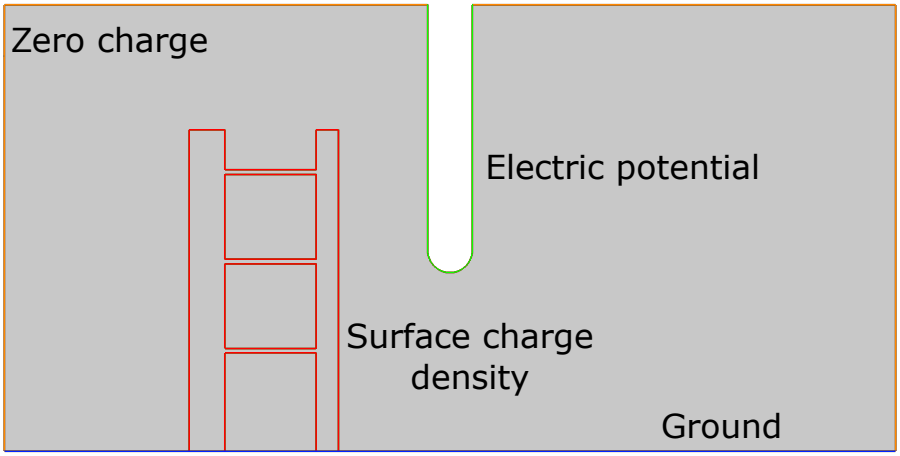

Figure 4.3: Electrostatic boundary conditions used approximate the electrostatic conditions.

5 | Results and discussions

This chapter presents and discusses relevant results for the research questions. The chapter is split into separate sections for each research question, and the sections are split into relevant aspects.

5.1 Surface-electrode distance effect

This section presents results relevant to the first research question, which focuses on how the distance between the surface and electrode affects breakdown.

5.1.1 Electrostatic simulations

To study the how the distance influences the electric field distortion, two electrostatic simulations were performed with distance from the electrode to the surface as a variable. The only difference between the simulations was the surface charges density.

The first simulation did not include surface charges to represent the initial condition of the surface. The second simulation assumed surface charge saturation to observe maximum field distortion. These two conditions are meant to represent the transient change in surface charge. Plots showing the electric field distribution from both simulations at 30 mm, 20 mm, and 10 mm are shown in Figure 5.1, Figure 5.2, and Figure 5.3 respectively. Comparing all three plots, there are a few interesting observations.

For all three distances at initial conditions, the field is very similar and only slightly affected by the surface. When the surfaces are charged, all distances exhibit the same behavior, with the field being pushed down to the lower half of the surface. However, the field is further enhanced as the surface is moved closer to the electrode. This is because the field becomes more tangential to the surface as it moves closer, therefore not being canceled out by the surface charges.

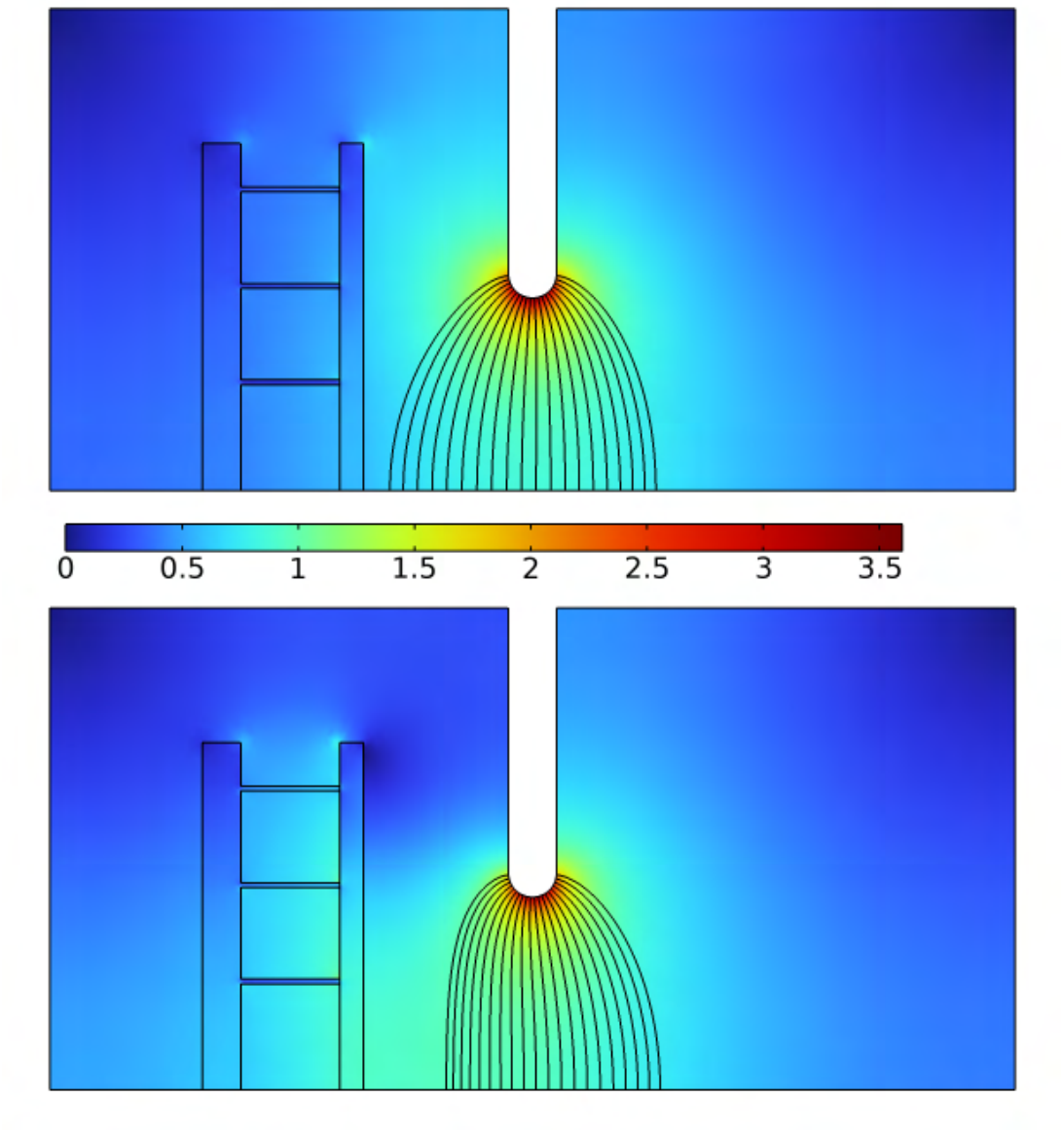

Figure 5.1: A plot of the electric field strength (kV/mm) and field lines with a distance between the electrode and surface of 30 mm both without surface charges (top) and with saturation charge (bottom).

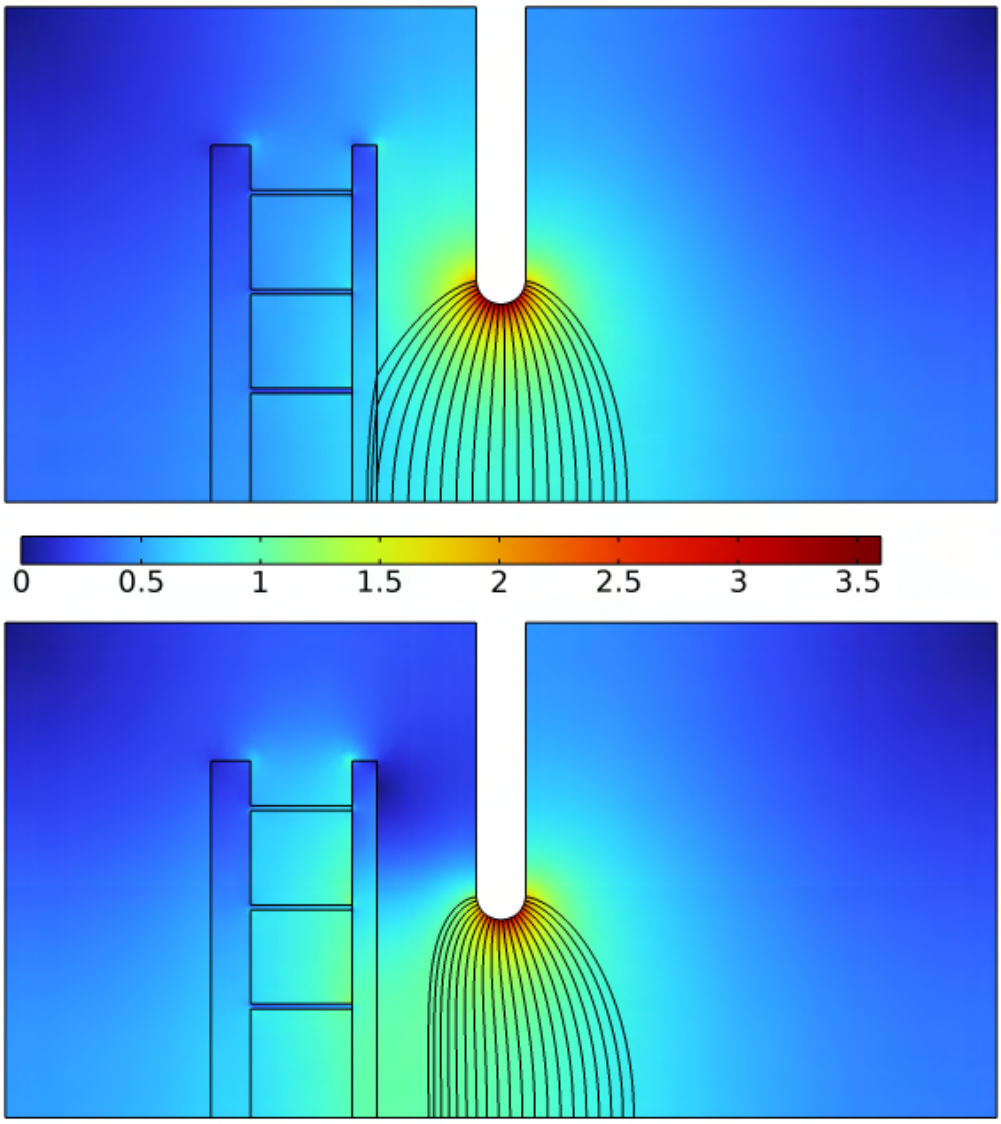

Figure 5.2: A plot of the electric field strength (kV/mm) and field lines with a distance between the electrode and surface of 20 mm both without surface charges (top) and with saturation charge (bottom).

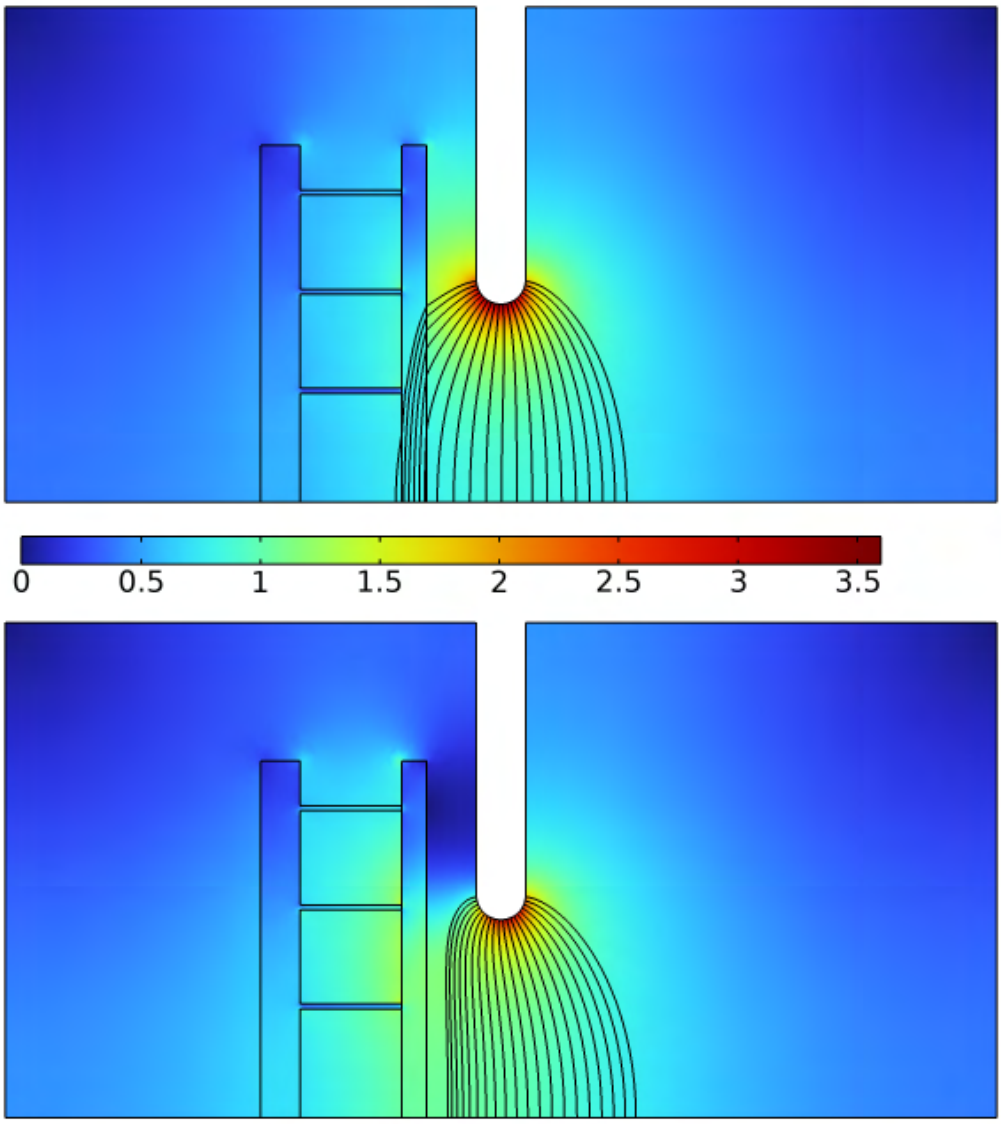

Figure 5.3: A plot of the electric field strength (kV/mm) and field lines with a distance between the electrode and surface of 10 mm both without surface charges (top) and with saturation charge (bottom).

5.1.2 Breakdown voltage

Up-and-down breakdown tests were performed to investigate how the air gap distance between the electrode and the polycarbonate will affect the breakdown voltage. An initial reference test was performed without the polycarbonate surface. The polycarbonate surface was then introduced at three different distances from the electrode. The results from all four tests are plotted in Figure 5.4, and the 50% breakdown voltages calculated using Equation 3.1 are presented in Table 5.1.

As may be seen from the results, the breakdown voltage is strongly dependent on the distance. The breakdown voltage increase appears to depend on at least two different effects that may dominate at different distances. One such effect may be the increasing tangential field close to the surface at decreasing distance. This may be counteracting the phenomenon responsible for increasing the breakdown voltage, which is still unknown.

The result of these counteracting effects is a potential optimal distance between the surface and electrode in which the breakdown voltage reaches a maximum. One might also hypothesise that this optimal distance would change depending on the air gap distance based on the field distribution in larger gaps.

Table 5.1: Calculated 50% breakdown voltages for positive impulses corrected using the voltage correction factor.

Distance [mm]	**$U_{50\%}$ [kV]**	**Increase in BD voltage compared to ref [%]**
Ref	61.2	-
10	64.8	5.9 %
20	81.4	33.0 %
30	66.2	8.2 %

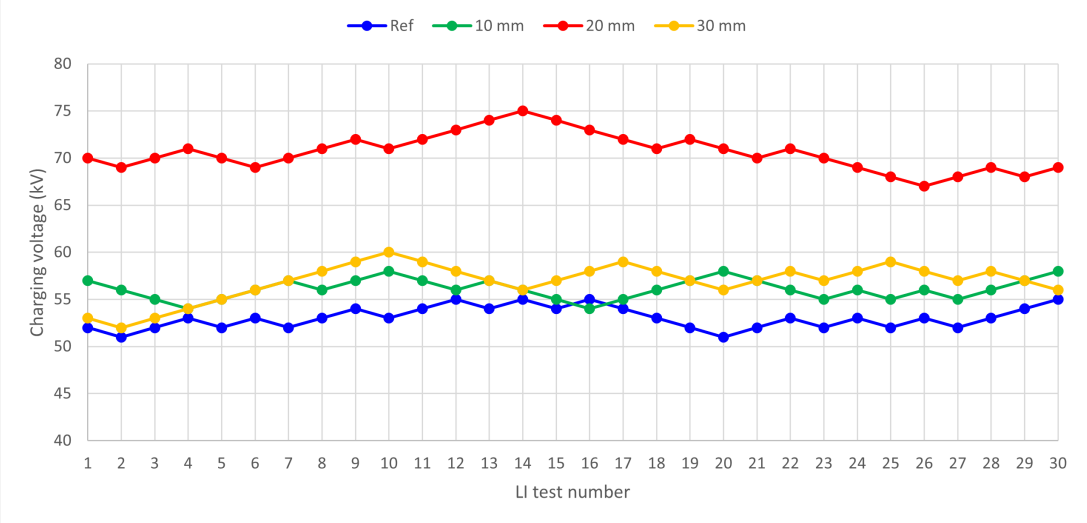

Figure 5.4: Results from Positive polarity up-and-down tests showing charging voltages (not corrected).

5.2 Breakdown voltage during fast negative voltage impulses

This section presents results relevant to the second research question, which focuses on how the parallel surface affects the breakdown voltage during fast

negative voltage impulses.

Electrostatic simulations are not presented in this section as they would be identical to the simulations in the previous section.

5.2.1 Breakdown voltage

Up-and-down tests were performed to investigate whether or not the polycarbonate has the same effect during negative fast lightning impulses. An initial reference test is performed without the polycarbonate present. The polycarbonate is then introduced at a distance of 20 mm from the electrode. This distance was chosen as it is the best distance for the effect of the distances tested for fast positive voltage impulses.The results from the two tests are presented in Figure 5.5, and the 50% breakdown voltages are presented in Table 5.2.

From these results, the parallel surface does not seem to affect the breakdown voltages during negative fast lightning impulses, as the change in breakdown voltage is within the margin of error for such a stochastic process. This may indicate that the effect observed for positive impulses is not present, or perhaps any counter effect is more prominent for negative impulses.

Table 5.2: Calculated 50% breakdown voltages for negative impulses corrected using the voltage correction factor.

Distance [mm]	**$U_{50\%}$ [kV]**	**Increase in BD voltage compared to ref [%]**
Ref	72.0	-
20	70.8	-1.7 %

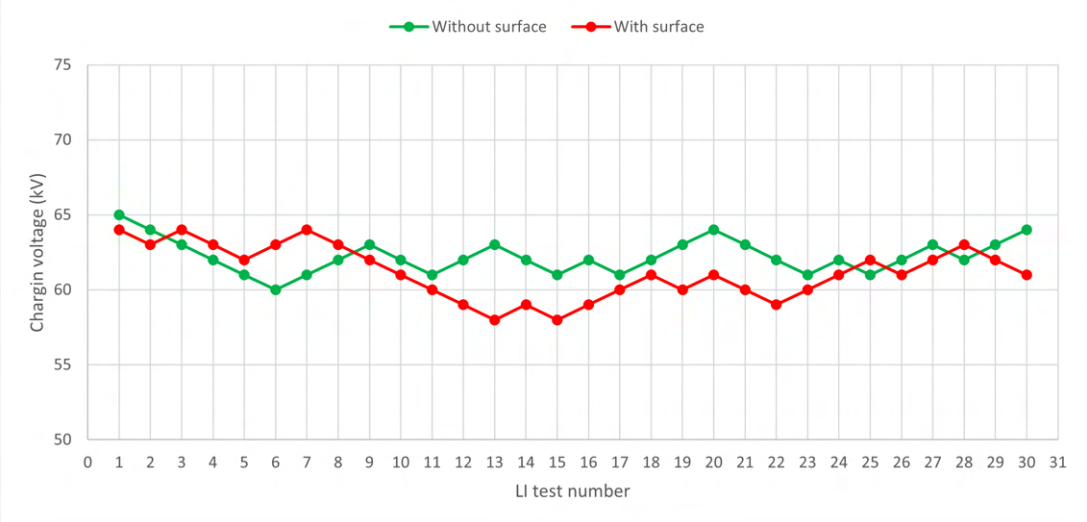

Figure 5.5: Results from negative polarity up-and-down tests showing charging voltages (not corrected) with positive polarity test as reference.

5.3 Discharge behavior parallel to a surface

This section presents images relevant to the third research question, which relates to how the parallel surface influences discharges in the air gap. An orange, segmented line is added to represent the surface position for all images where the surface is present but not obvious.

5.3.1 Positive streamer discharges

Positive streamer discharges are the first discharges of interest as they are the lowest voltage discharges being investigated and are also the precursor to leader discharges, as discussed in section 2.2. The streamer discharges also propagate without any initial surface charges.

Two representative images captured using the Lambert HiCam are shown in Figure 5.6, one being a reference image without the surface and one with the surface present.

Based on the images captured, the streamers do not appear to be affected by the parallel surface other than being physically blocked by it. This is an expected result based on the simulations of the electric fields shown in Figure 5.2, where the field before surface charging is non-distorted.

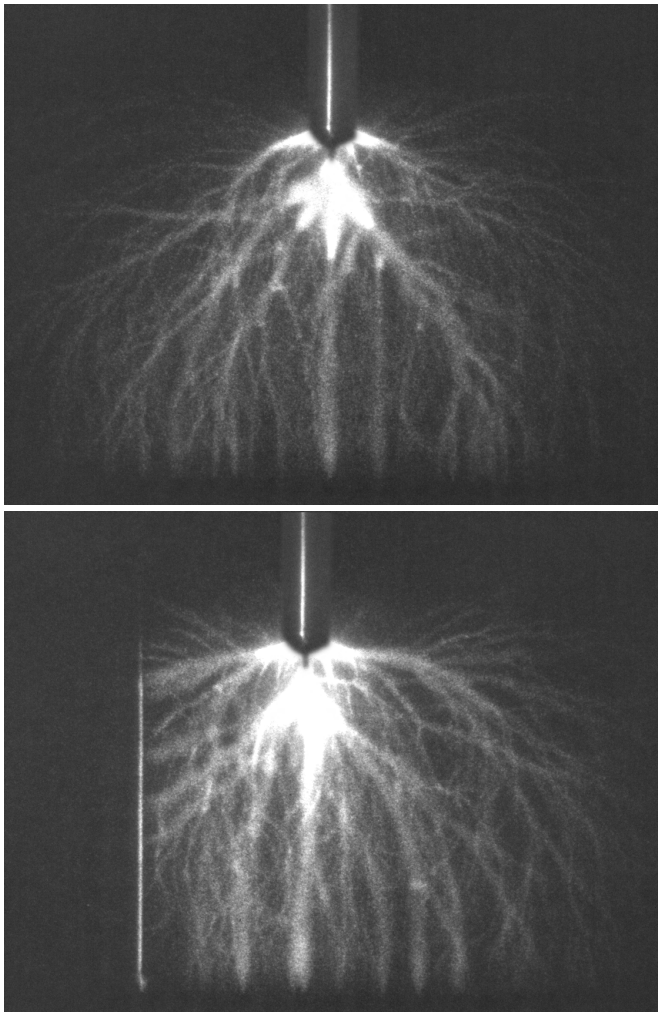

Figure 5.6: Images of streamer discharges captured using HiCam. Top image without parallel surface and bottom image with the parallel surface. Charging voltages: 42 kV and 50 kV respectively. Exposure time: 200 μs.

5.3.2 Positive leader discharges

Positive leader discharges are the second discharges of interest. As leaders will have significantly higher conductivity, as discussed in section 2.2, the leader discharges may increase the distortion caused by the surface even further. Four image series are presented to discuss four different observed effects affecting leader discharges.

The first image series, Figure 5.7, shows two separate leader channels: the left leader channel moves close to the surface, and the right leader channel moves away from the surface. Initially, both seem to be propagating at almost the same rate; however, the left leader channel begins to propagate further in frame 4. In frame 5, the left leader channel appears to get dimmer and has not propagated any further than in frame 4. The leader channel then begins to die out. As the

left leaders channel dies out, the right leader channel continues to propagate and will most likely end in a breakdown.

This is one of the trends observed in multiple image series in which two or more leaders channels are initiated. If one leader channel propagates close to the surface and one propagates further away, the one further away appears to always be the one leading to breakdown.

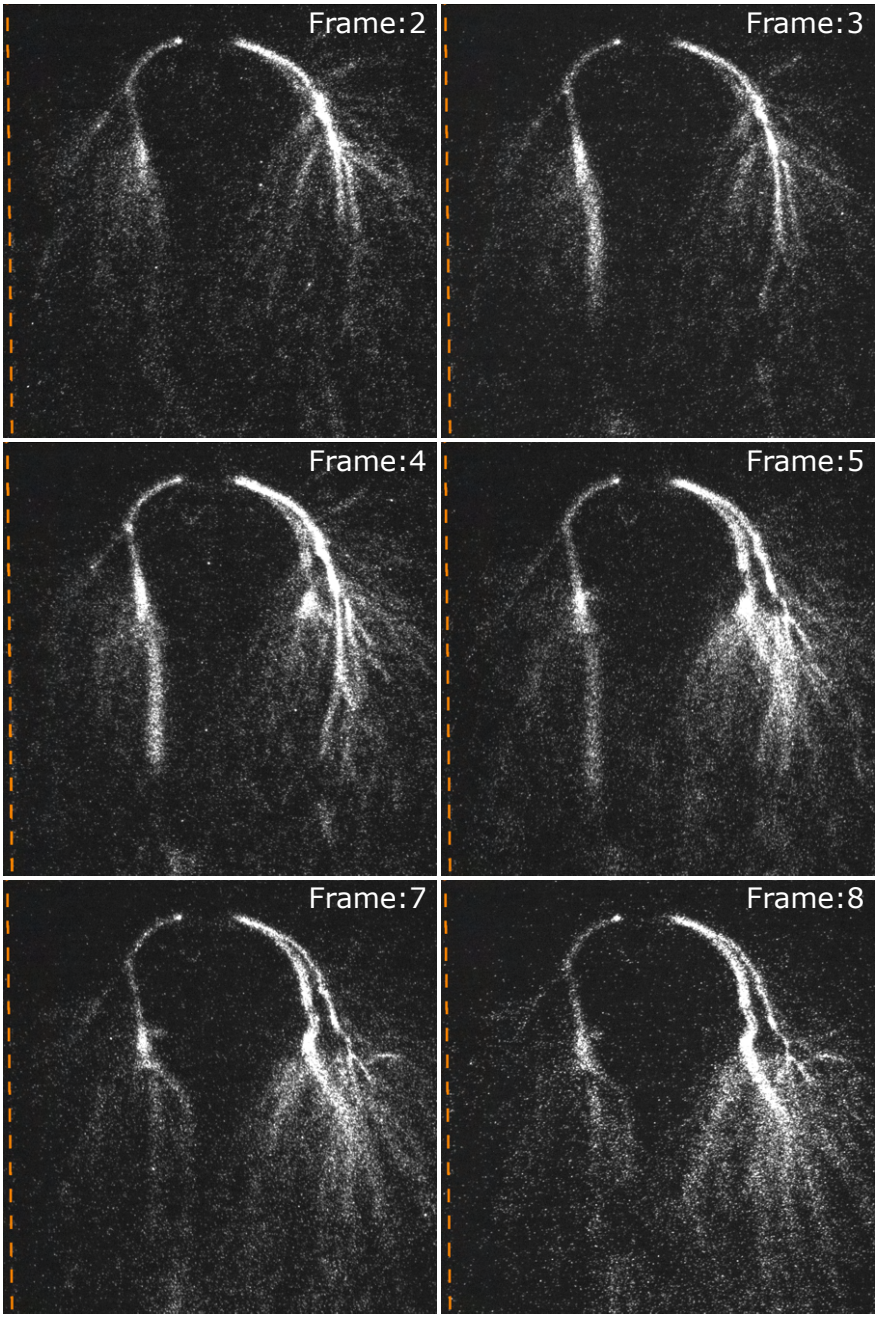

Figure 5.7: Image series captured using SIMX16 showing two "competing" leader discharges. Charging voltage: 65 kV. Distance between surface and electrode: 20 mm. Exposure time per frame: 20 ns.

The second images series, Figure 5.8, shows a situation where only a single leader channel has been able to propagate before the first frame. However, the leader channel does not appear to be able to propagate further toward the ground plane. As the left leader channel is unable to propagate further, a second leader channel begins to develop on the right side of the image, away from the surface. This new leader channel begins to propagate and is expected to bridge the gap and cause breakdown.

This is also an occurrence that has been observed a few times, although not as often as the previously mentioned situation above. It is still unclear how the leader channel is able to stay almost stationary in space without dying out.

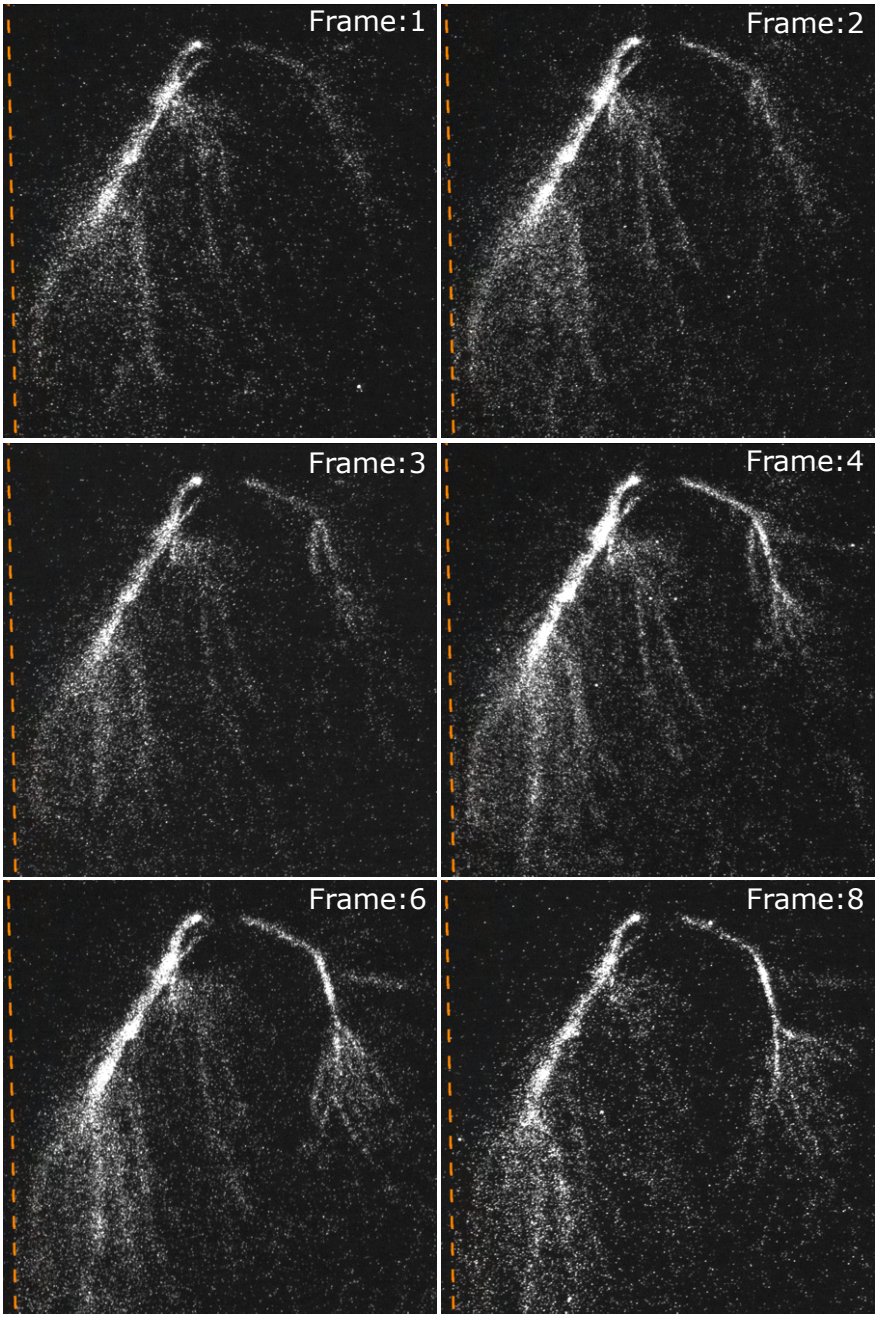

Figure 5.8: Image series captured using SIMX16 showing a leader channel propagation being halted. Charging voltage: 65 kV. Distance between surface and electrode: 20 mm. Exposure time per frame: 10 ns.

The third image series, Figure 5.8, shows the most common occurrence of leader discharges. In this situation, one or more leader channels are initiated away from the surface. In this specific image series, one leader propagates on the right side furthest away from the surface, and the other appears to propagate on the far side of the electrode into the image plane.

In these situations, the leader channels appear to propagate fast and unimpeded, as well as following typical field lines as shown in Figure 5.2.

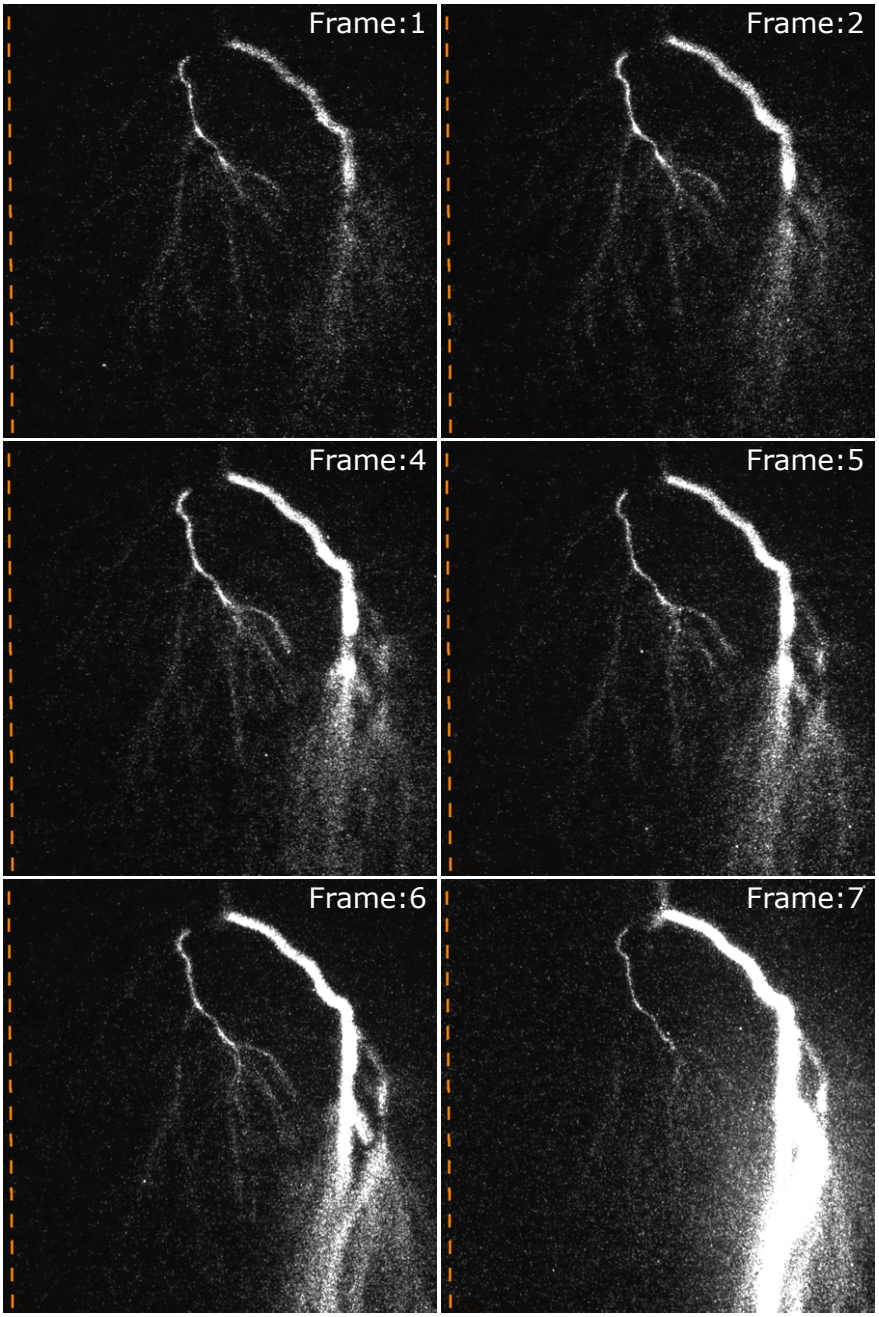

Figure 5.9: Image series captured using SIMX16 a leader discharge propagating freely. Charging voltage: 65 kV. Distance between surface and electrode: 20 mm. Exposure time per frame: 10 ns.

The final image series, Figure 5.10, shows an occurrence currently only observed when the surface is placed 10 mm away from the electrode. In this situation, a leader channel has initiated at the electrode on the side facing away from the

surface. The leader then begins to propagate towards the surface, but its propagation is halted close to the ground plane. After multiple frames, a second leader channel is able to branch out from the body of the original leader channel and propagates further away from the surface. This leader channel is then able to fully bridge the gap and cause breakdown, as seen in the last frame of Figure 5.10.

Based on the distance to the surface and the fact that the original leader channel already initiated on the right side of the electrode, the branching might be because this is the furthest point away from the surface where it may be initiated.

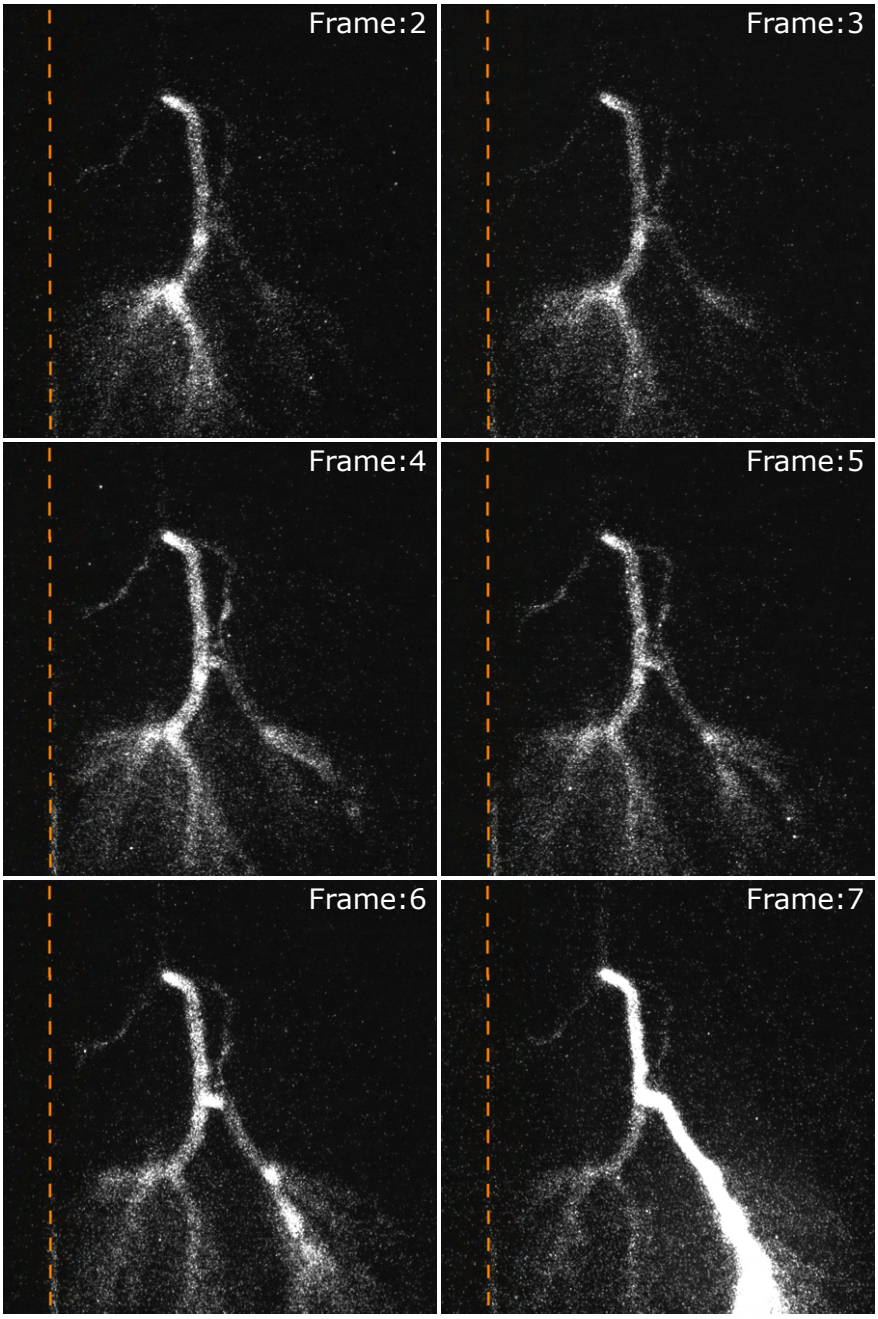

Figure 5.10: A branching leader discharge developing as the primary leader channel stops propagating. Charging voltage: 55 kV. Distance between surface and electrode: 10 mm. Exposure time per frame: 20 ns.

Based on the images captured of leader discharges, it is clear that positive leaders are significantly affected by the surface, specifically the surface charges. Comparing the four situations described above, the cause appears to be the same where the field close to the surface and ground is significantly weakened.

One potential hypothesis of this field weakening may be a significant increase in

surface charge, which may be even higher than saturation charge due to the high conductivity of the leader channels. As the a leader channels propagates close to the surface, the potential of the electrode will move with the leader channel [7]. This may increase the normal field into the surface, and therefor increase the maximum surface charge density. Based on the field strength observed between the electrode and surface in the simulations in Figure 5.2, the field may become too weak to facilitate leader propagation.

5.3.3 Negative discharges

Images of negative streamer discharges were also captured to investigate how these were affected by the parallel surface. As was shown in section 5.2, the surface does not appear to affect the breakdown voltage for fast negative impulses, but discharges may still be affected. Multiple attempts to capture images of negative leader discharges were performed, but none succeeded.

Based on images captured using the Lambert HiCam, negative streamers do not appear to be affected when a breakdown does not occur. Figure 5.11 show four separate images of negative streamer discharges, and none of them appear to interact at all with the surface. However, this does not appear to be the case when a breakdown is about to occur.

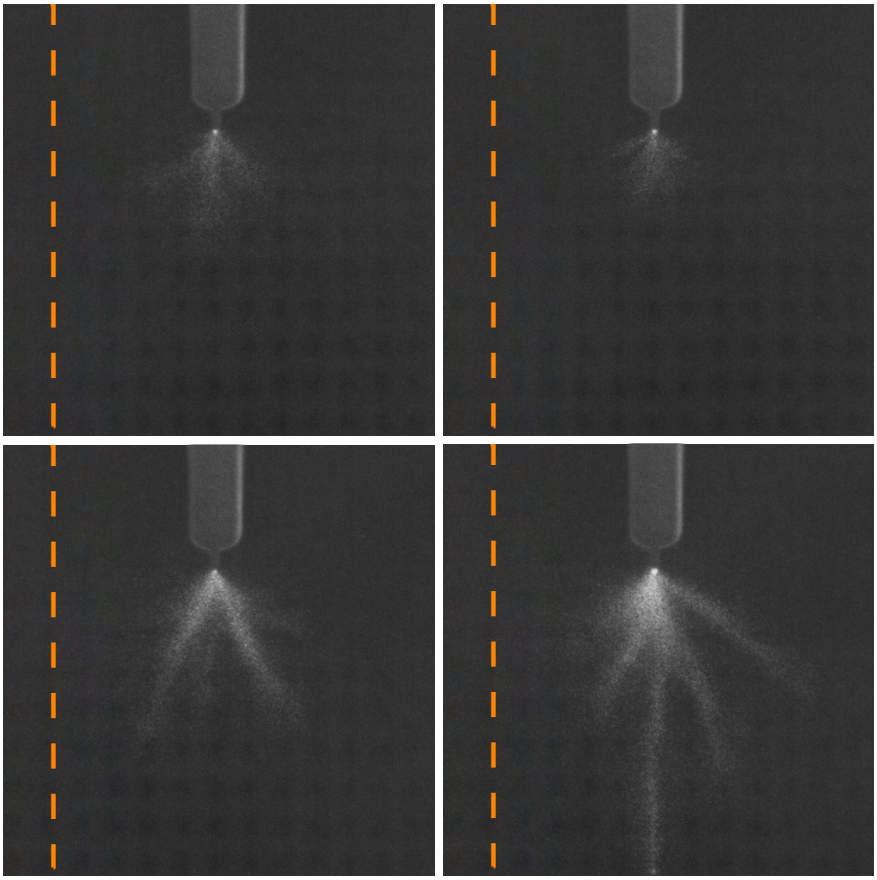

Figure 5.11: Four examples of negative streamer discharges captured using HiCam. Charging voltages: 40 kV, 40 kV, 44 kV and 46 kV respectively. Exposure time: 200 μs.

In Figure 5.12, secondary streamer discharges appear to be originating from both the ground plane (blue circle) and from the surface itself (red circle). A later frame from the same image series is shown in Figure 5.13. It shows that the streamer discharges emanating from the surface have further developed and are now the main discharges occurring in the gap. It is clear that negative discharges behave very differently from positive discharges and interacts with the surface in what appears to be the exact opposite way.

Exactly why this occurs is out of the scope of this thesis but is something of interest that may be explored in further experiments.

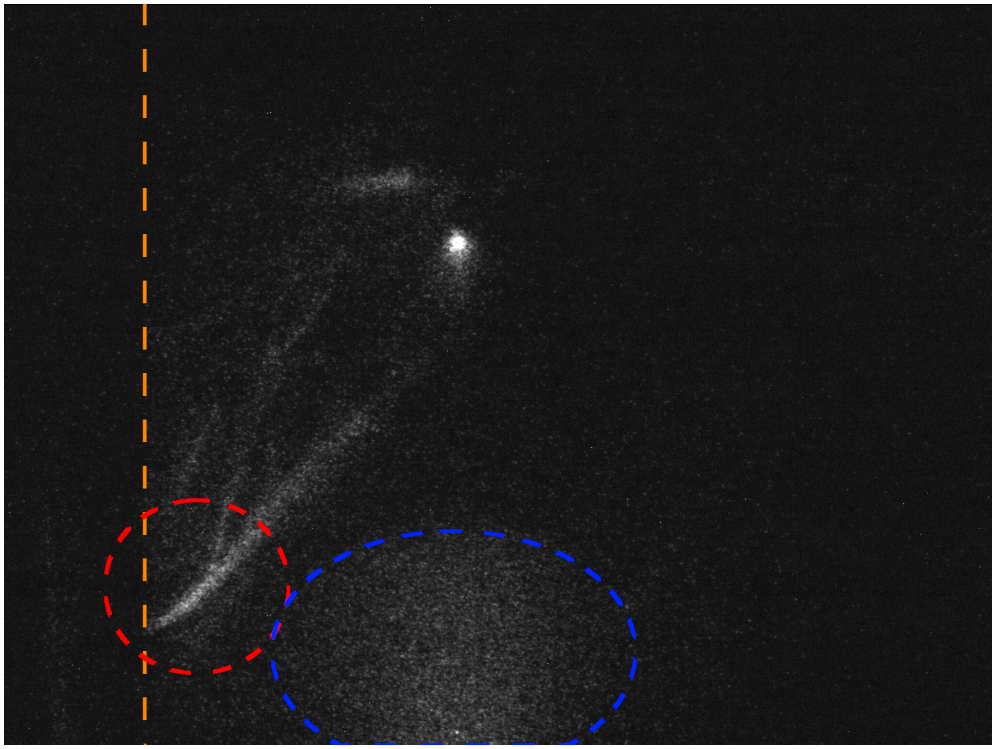

Figure 5.12: Long exposure image captured using SIMX16 of streamers prior to breakdown. Charging voltage: 70 kV. Exposure time: 720 ns.

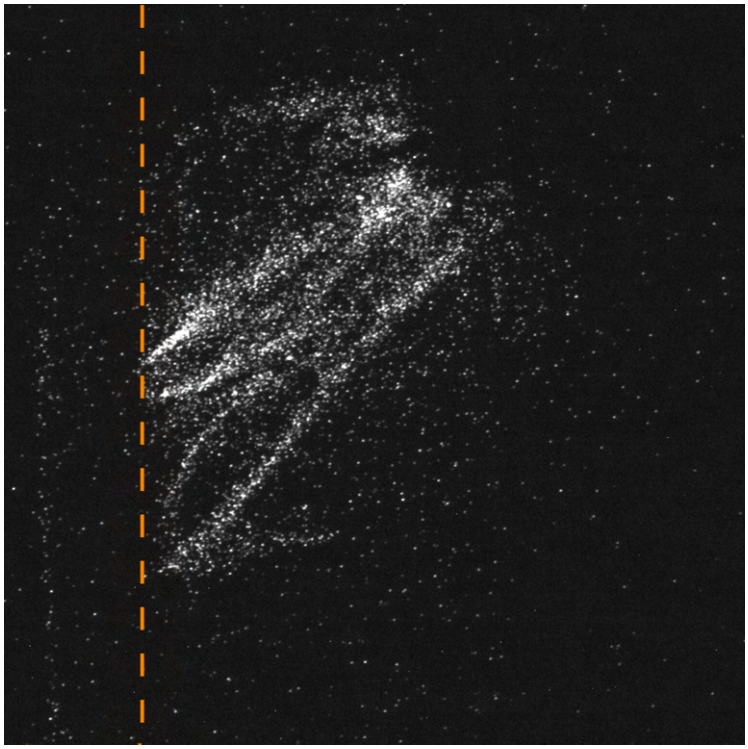

Figure 5.13: SIMX16 image of pre-breakdown negative discharges shortly before breakdown. Charging voltage: 70 kV. Exposure time: 20 ns.

5.4 AC testing of evaporated carbon layer

This section presents the results from the AC experiments that are relevant to the final research question. The two main questions are whether or not the carbon layer is conductive enough to reduce the AC breakdown voltage of a gap and if the carbon layer is thick enough to produce excess heating.

5.4.1 Breakdown voltage

One of the most critical factors when including anything in a test setup is that it cannot influence the tests in any significant way, especially for alternative gas testing, where it cannot affect the breakdown voltage.

Based on the breakdown tests, the breakdown voltage decreased by 1.5 kV, as shown in Table 5.3 and Figure 5.14. This small change in breakdown voltage may point to the carbon layer affecting the electric field, as it was also visually observed that the breakdown channel was attracted to the bottom of the surface. However, because the change is small, the decrease may also be caused by small changes in the test setup occurring while placing the surface and its bracket parallel to the electrode.

Based on this initial test and its sources of error, the surface does not affect the breakdown voltage significantly. This means that the carbon layer is potentially suitable for tests involving AC but should be further investigated and refined based on the application. The current main application for this strategy is impulse testing, but such tests may also include AC.

Table 5.3: The average AC breakdown voltage of the test object with and without the parallel surface.

Transformer ratio 0.23/110 kV		
	Variac voltage [V]	**HV [kV]**
Without surface	84.9	40,6
With surface	81.7	39.1

Figure 5.14: Plot of the results from the AC breakdown tests.

5.4.2 Surface heating

Throughout the breakdown voltage tests, the infrared camera showed no increase in surface temperature. The temperature fluctuated in the 18-20 °C range throughout the experiments, but this may be attributed to the temperature in the room and some uncertainty in the calibration of the camera. A more accurate temperature reading may have been possible by moving the camera closer, but this was not possible as this would have put the camera too close to high voltage. This was also not deemed necessary, as the temperature change is at worst within a degree or two.

6 | Conclusion

Based on the results presented and discussed in this thesis, a few conclusion pertaining to the four research question may be drawn. The main conclusion from each research question will be presented in the order the questions were posed in the introduction (section 1.2).

1. The electric field distortion is minimal when there are no surface charges present. However, the distortion is significant when the surface is saturated and the distortion increases with smaller distance. The breakdown voltage for fast positive lightning impulses are heavily dependent on the distance between the surface and the electrode. At very close distances, the breakdown voltage is only slightly increased. As the surface is moved further away, the breakdown voltage increases significantly with an observed increase of 33%. This increase in breakdown voltage will then decrease as the surface is moved further away. Together, this indicates an optimal distance at which the breakdown voltage increase is at its maximum.

2. The breakdown voltage for fast negative lightning impulses does not appear to be affected by the presence of a parallel surface.

3. A parallel surface does not appear to affect positive streamer discharges in any significant way, but does affect positive leader discharges. Positive leader discharges propagating close to the lower part of the surface will not be able to reach the ground plane and other leader discharges moving further away from the surface will instead be allowed to propagate until breakdown.
   Negative streamer discharges were shown to be shown to also be significantly affected, as secondary streamer discharges were observed emanating from the surface.

4. The evaporated carbon layer applied to the parallel surface did not exhibit any significant negative effects during AC application. The breakdown voltage did decrease slightly, but was within margin of error and may therefor be a result of other variables. The surface also did not show any observable rise in temperature during testing.

7 | Further work

Three of the four research questions were all related to different aspects of the same phenomena, and further research is required to acquire a deeper understanding of its mechanisms.

Some of the future research may include:

- Measuring surface charges following a breakdown to get a better picture of surface charge distribution.
- As much of the electromagnetic radiation emitted by discharges is in the UV spectrum, using a UV sensitive lens may yield better images.
- Due to the big difference in gas pressure inside streamer- and leader discharges, Schlieren imaging may be used to study leaders more clearly without streamer discharges interfering [6].
- Stereoscopic imaging could be used to obtain a more complete picture of the discharges.
- Performing the same experiments in other insulating gases could shine more light on differences in discharge behaviors between gases.
- To try to maximize the surface area and surface charges, one option would be to switch out the polycarbonate surface with aerogel to observe how the increase in surface area may affect the results.
- Including multiple surfaces around the electrode.

To further investigate aspects of the evaporated carbon layer on the polycarbonate sheet, some further work may include:

- Attempt to measure surface charge decay and how long it takes to be completely free of charges after an impulse.
- Perform tests with different carbon layer thicknesses/surface conductivity to observe how this affects performance.

References

[1] Stian Nessa. *New Environmentally-friendly Insulation Gases: Breakdown Mechanisms near Insulating Surfaces*. Unpublished. 2021.

[2] Sander Nijdam, Jannis Teunissen, and Ute Ebert. *The physics of streamer discharge phenomena*. May 2020.

[3] C. Montijn. "Evolution of negative streamers in nitrogen : a numerical investigation on adaptive grids". English. PhD thesis. Applied Physics, 2005. ISBN: 90-386-2371-2. DOI: 10.6100/IR598717.

[4] Alejandro Luque et al. "Photoionization in negative streamers: Fast computations and two propagation modes". In: *Applied Physics Letters* 90.8 (2007), p. 081501. DOI: 10.1063/1.2435934. eprint: https://doi.org/10.1063/1.2435934. URL: https://doi.org/10.1063/1.2435934.

[5] Joshua Yoskowitz et al. "New Simulations for Ion-Production and Back-Bombardment in GaAs Photo-guns". In: Sept. 2020, p. 040. DOI: 10.22323/1.379.0040.

[6] Xiangen Zhao et al. *Elongation and branching of stem channels produced by positive streamers in long air gaps*. https://doi.org/10.1038/s41598-021-83816-7. 2021.

[7] Hans Kristian Meyer et al. "Surface charging of dielectric barriers in short rod-plane air gaps-experiments and simulations". In: *2018 IEEE International Conference on High Voltage Engineering and Application (ICHVE)*. 2018, pp. 1–4. DOI: 10.1109/ICHVE.2018.8642108.

[8] Hans Kristian Hygen Meyer. "Dielectric barriers under lightning impulse stress. Breakdown and discharge-dielectric interaction in short non-uniform air gaps". PhD thesis. Norwegian University of Science and Technology, Mar. 2019.

[9] Atle Pedersen and Andreas Blaszczyk. "An engineering approach to computational prediction of breakdown in air with surface charging effects". In: *IEEE Transactions on Dielectrics and Electrical Insulation* 24.5 (2017), pp. 2775–2783. DOI: 10.1109/TDEI.2017.006650.

[10] International Electrotechnical Commission (IEC). *IEC 60060-1:2010 High-voltage test techniques - Part 1: General definitions and test requirements*. 2010.

[11] E. Kauffel, W.S.Zaengl, and J. Kuffel. *High Voltage Engineering*. second. Butterworth-Heinemann, 2000.

[12] W. Hauschild et al. *Statistical Techniques for High-voltage Engineering*. Energy Engineering Series. P. Peregrinus, 1992. ISBN: 9780863412059.

A | Results from previous work

This appendix is added to present some results from previous work that may be of interest to the discussion in this thesis.

A.1 How pre-existing surface charges affects breakdown voltage

Table A.1: Estimated 50% breakdown voltages from tests T1, T2 and T3.2 [1].

Test name	**Estimated 50% breakdown voltage**
T1	47 kV
T2	49.5 kV
T3.2	63 kV

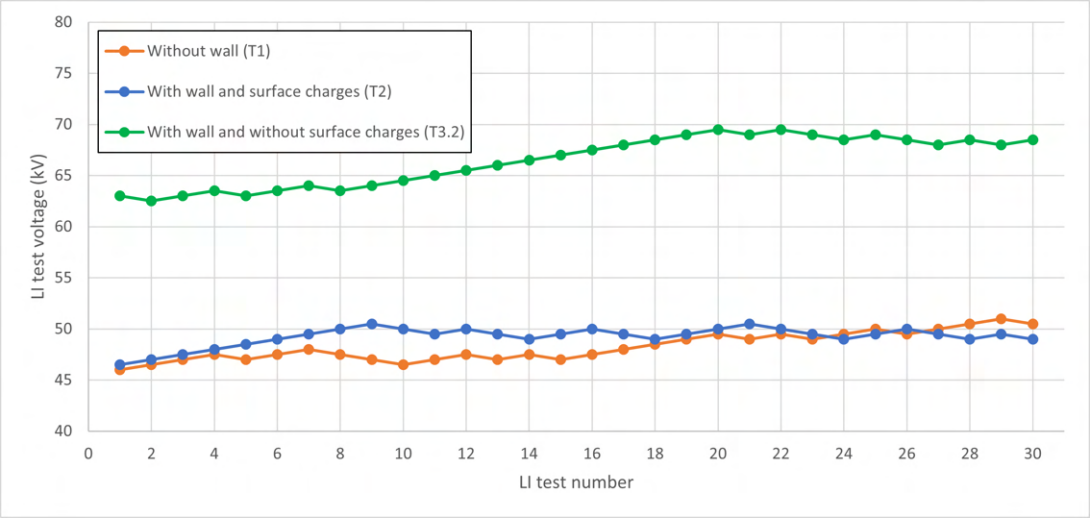

Figure A.1: Graph showing results from up and down tests with test procedures T1, T2, and T3.2 [1].

A.2 Surface charge removal by evaporated carbon

Table A.2: Estimated 50% breakdown voltages from tests T1, T3.2 and T6 [1].

Test name	Estimated 50% breakdown voltage
T1	47 kV
T3.2	63 kV
T6	64 kV

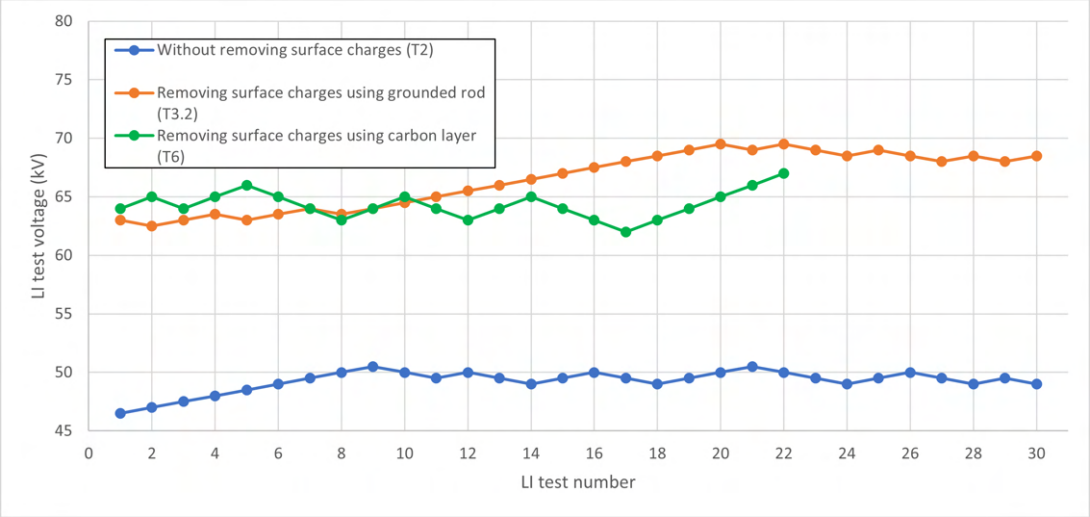

Figure A.2: Graph showing results from up and down tests with test procedures T1, T3.2, and T6 [1].

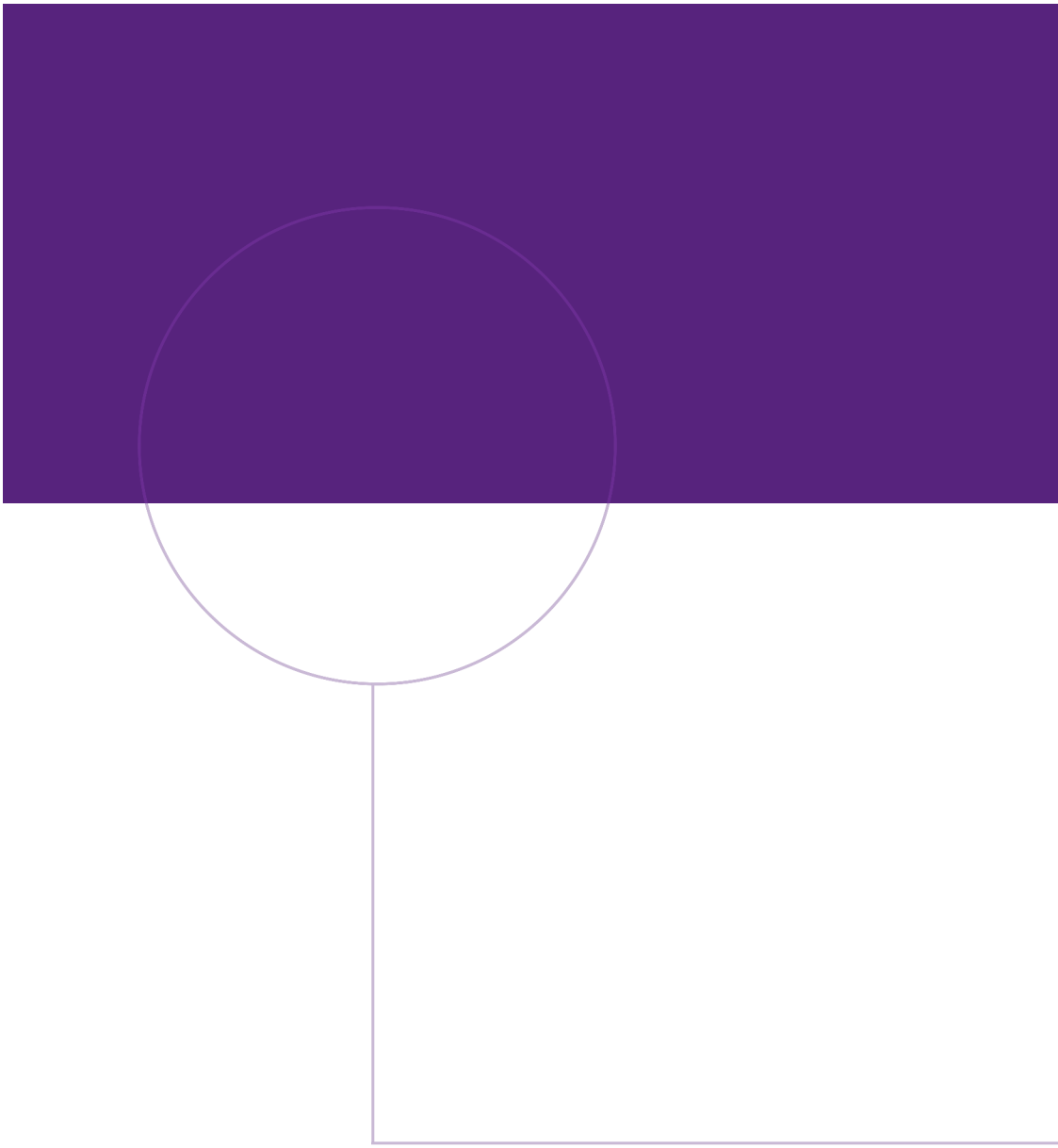

NTNU

Norwegian University of
Science and Technology